Available online at www.sciencedirect.com

ScienceDirect

Developmental Biology 299 (2006) 176–192

DEVELOPMENTAL BIOLOGY

www.elsevier.com/locate/ydbio

Parcas, a regulator of non-receptor tyrosine kinase signaling, acts during anterior–posterior patterning and somatic muscle development in *Drosophila melanogaster*

Karen Beckett, Mary K. Baylies *

Program in Developmental Biology, Sloan-Kettering Institute, Memorial Sloan-Kettering Cancer Center, Weill Graduate School of Medical Science at Cornell University, 1275 York Avenue, New York, NY 10021, USA

Received for publication 14 December 2005; revised 10 July 2006; accepted 19 July 2006
Available online 11 August 2006

Abstract

We have isolated *parcas* (*pcs*) in a screen to identify novel regulators of muscle morphogenesis. Pcs is expressed in the ovary and oocyte during oogenesis and again in the embryo, specifically in the developing mesoderm, throughout muscle development. *pcs* is first required in the ovary during oogenesis for patterning and segmentation of the early *Drosophila* embryo due primarily to its role in the regulation of Oskar (Osk) levels. In addition to the general patterning defects observed in embryos lacking maternal contribution of *pcs*, these embryos show defects in Wingless (Wg) expression, causing losses of Wg-dependent cell types within the affected segment. *pcs* activity is required again later during embryogenesis in the developing mesoderm for muscle development. Loss and gain of function studies demonstrate that *pcs* is necessary at distinct times for muscle specification and morphogenesis. Pcs is predicted to be a novel regulator of non-receptor tyrosine kinase (NRTK) signaling. We have identified one target of Pcs regulation, the *Drosophila* Tec kinase Btk29A. While Btk29A appears to be regulated by Pcs during its early role in patterning and segmentation, it does not appear to be a major target of Pcs regulation during muscle development. We propose that Pcs fulfils its distinct roles during development by the regulation of multiple NRTKs.

Keywords: Parcas; Oskar; Wingless; Btk29A; Non-receptor tyrosine kinase signaling; Mesoderm; Muscle; Morphogenesis

Introduction

A common theme throughout the development of all multicellular organisms is the redeployment of individual genes or gene cassettes at different times and places. Genes may be required for development of several tissues within an organism or at multiple times within development of a specific tissue. One model system that has proved highly fruitful in the study of pleiotrophic genes is *Drosophila melanogaster* due to the power of both classical genetics and clonal analysis. In particular, this system has allowed the identification of several signaling pathways that are used reiteratively throughout development (Lai, 2004; Simon, 2000). Although much is now known about the molecular components that build these signaling pathways, how time and tissue context affect their final output is still not well understood. It is apparent, however, that the output of signaling pathways may be influenced by positive and negative regulatory proteins that are expressed in a temporal and tissue specific manner (e.g. Panin and Irvine, 1998).

The mesoderm of the *Drosophila* embryo has provided an excellent system to study the reiterative use of signaling pathways during development (Baylies and Michelson, 2001; Baylies et al., 1998; Frasch, 1999). This germ layer gives rise to a number of tissues, most notably the larval body wall muscles, through the integration of multiple signal transduction pathways. There are thirty body wall muscles in each embryonic hemisegment. Each body wall muscle has a unique size, shape, orientation, attachment sites in the epidermis, and innervation by the nervous system. Body wall muscles arise from two cell types specified in the somatic mesoderm, founder cells (FCs) and fusion competent myoblasts (FCMs). FCs contain all the information required to form an individual muscle (Bate, 1990; Dohrmann et al., 1990). Upon fusion to an FC, FCMs become

* Corresponding author. Fax: +1 646 422 2355.
E-mail address: m-baylies@ski.mskcc.org (M.K. Baylies).

0012-1606/$ - see front matter © 2006 Elsevier Inc. All rights reserved.
doi:10.1016/j.ydbio.2006.07.049

entrained to that particular muscle program. The identification of FCM-enriched genes that regulate muscle morphogenesis, however, suggested that FCMs may not be the naive cell type that previous studies have indicated (Artero et al., 2003; Estrada et al., 2006). In addition, other observations have suggested that FCMs are not a uniform population of myoblasts (Artero et al., 2001; Estrada et al., 2006; Ruiz-Gomez et al., 2002). For example, *hibris* (*hbs*), an Ig-domain containing protein required for fusion, is expressed only in a subset of FCMs (Artero et al., 2001). Together, these data indicated that FCMs are a diverse population of myoblasts that contribute specific information to muscle fusion and morphogenesis.

We identified *parcas* (*pcs*; also known as *poirot*) in a microarray screen to identify novel genes required for muscle morphogenesis (Artero et al., 2003). Data from the microarray screen predicted that Pcs would be enriched in FCMs and was likely to be important in muscle morphogenesis. *Pcs* is the *Drosophila* orthologue of the mammalian gene Sab. Sab (*S*H3-domain binding protein that preferentially *a*ssociates with *B*tk) was identified as a novel protein that binds to the SH3 domain of BTK (*B*ruton's *t*yrosine *k*inase) in vitro (Matsushita et al., 1998). Sab associates with BTK in vivo and negatively regulates its activation (Yamadori et al., 1999), but the mechanism of this regulation is not well understood. BTK is a member of a family of non-receptor tyrosine kinases called Tec kinases. These kinases play roles in multiple processes including cell survival, proliferation, differentiation, and cytoskeletal regulation (Lewis et al., 2001; Smith et al., 2001). There is only one member of this family of proteins in *Drosophila*, Btk29A (also known as Tec29). The principle role of this protein in *Drosophila* development to date is in regulation of the actin cytoskeleton during ring canal growth in oogenesis, cellularization, salivary gland invagination, and dorsal closure (Chandrasekaran and Beckendorf, 2005; Guarnieri et al., 1998; Roulier et al., 1998; Tateno et al., 2000; Thomas and Wieschaus, 2004).

Previous studies on Pcs have focused on its role and interaction with Btk29A during oogenesis (Sinka et al., 2002). These studies demonstrated that Pcs is required for the specification of posterior cell types during anterior–posterior (A–P) patterning early during embryogenesis. The establishment of A–P polarity in early *Drosophila* embryos depends upon gradients of maternally deposited factors (Johnstone and Lasko, 2001; Riechmann and Ephrussi, 2001). One of these factors, Nanos (Nos), is specifically required to determine posterior structures within the embryo (Lehmann and Nusslein-Volhard, 1991; Wang and Lehmann, 1991). Nos protein is distributed in a gradient along the A–P axis of the embryo, with its highest levels at the posterior pole. This gradient of Nos is due to the specific translation of its transcript at the posterior pole of the embryo by multiple factors, including the protein Oskar (Osk), and the subsequent diffusion of Nos protein away from its source (Gavis and Lehmann, 1992; Wang et al., 1994). For Osk to localize *nos* to the posterior pole of the embryo, it too has to be localized correctly (Ephrussi et al., 1991). Although *osk* mRNA is localized posteriorly during oogenesis, it is the translation and post-translational regulation of this transcript that has been shown to establish wild type *osk* activity at the posterior pole. Several genes have been identified that are required specifically for the localization of Osk protein (Jankovics et al., 2001, 2002). Of these, *pcs* is required for localization of Osk protein, but not its mRNA. Embryos laid by *pcs* homozygous mutant mothers showed a reduction and delocalization of Osk (Sinka et al., 2002). As a result, these embryos lack the most posterior structures of the embryo, the pole cells, and therefore are sterile.

Here, we report that *pcs* is used reiteratively during development of the *Drosophila* embryo and that these different roles have significant ramifications for the development of the larval body wall muscles. First, *pcs* is required maternally to establish correct anterior–posterior patterning, which in turn regulates subsequent mesoderm development. This appears to be due primarily to the role of Pcs in regulation of Osk expression levels during oogenesis. Embryos lacking maternal *pcs* expression show disruptions in embryonic patterning. A subset of these defects are due to losses of Wingless (Wg) expression and thus the specification of Wg-dependent cell types within the developing embryo. Second, we show that *pcs* is required later, specifically in the mesoderm, for both muscle specification and morphogenesis. This requirement for Pcs at several steps of muscle development is consistent with its expression in the mesoderm throughout muscle development. While the *Drosophila* Tec kinase Btk29A appears to be the major target of Pcs regulation during early patterning events, we also demonstrate a lack of Btk29A expression and activity during muscle development, suggesting that Pcs has additional targets. We therefore propose that Pcs fulfils these different roles during embryonic development by regulating the activity of multiple non-receptor tyrosine kinases.

Materials and methods

Drosophila genetics

Crosses were performed at 25°C unless otherwise stated. *yw* was used as the wild type strain. Fly stocks were: pcs^{gs} (provided by M. Erdélyi); N^{55e11} and *UAS-*N^{intra} (provided by T. Lieber); *UAS-*ras^{N17}, *UAS-*ras^{V12}, and *twi-GAL4; Dmef2-GAL4* (provided by A. Michelson); $Btk29A^{k00206}$ (Roulier et al., 1998); *rP298* (Ruiz-Gomez et al., 2000); *twi-CD2* (Borkowski et al., 1995); *prd-GAL4* (Brand and Perrimon, 1993); *UAS-ΔNTCF* (van de Wetering et al., 1997), *oskM139L*, osk^{54}, and *Df(3R)pXT103* (a gift from Anne Ephrussi). osk^{301} is a temperature sensitive allele. Embryos laid by females homozygous for this allele at 18°C show posterior localization of *osk* mRNA and weak abdominal defects. osk^{CE4} is a stronger allele, and embryos laid by females homozygous for this allele show no *osk* mRNA at the posterior pole and are agametic (Ephrussi et al., 1991). *OskM139L* is a transgene that expresses the long isoform of Osk only (Markussen et al., 1995). osk^{54} contains a nonsense codon in the amino-terminal region and does not produce any Osk protein. *Df(3R)pXT103* uncovers *osk* (Kim-Ha et al., 1991). Combinations of mutations and stocks required for overexpression experiments were generated by standard genetic crosses at 25°C. For phenotypic studies, relevant stocks were balanced with *CyO P[*w^+ *ftz-lacZ], TM3 Sb Ubx-lacZ* or *FM7 P[*w^+ *ftz-lacZ]*. GAL4/UAS experiments were performed at 25°C or 29°C as noted.

Germline transformation and constructs

Pcs protein was overexpressed using the GAL4/UAS system (Brand and Perrimon, 1993). Full length *pcs* cDNA (GH09755) was subcloned into pBluescript SK+ (pBS) by PCR using 5′ primers containing a *Sma*I site

(TCCCCCGGGAATGTCGAGT) and 3′ primers containing an *Eco*RI site (CCGGAATTCACTATTCCAGAGAGCG). This *pcs* cDNA was subcloned from pBS into the overexpression construct pUAST using *Xba*I and *Eco*RI. The *pcs* RNAi construct was made by first subcloning a 500 bp fragment of GFP DNA downstream of the *pcs* cDNA in pBS-pcs using *Hin*dIII. The second copy of the *pcs* cDNA was subcloned into this construct by PCR using 5′ primers containing a *Kpn*I site (CGGGGTACCACTATTCCAGAGAGCG) and 3′ primers containing a *Xho*I site (CCGCTCGAGAATGTCGAGT). This resulted in pBS containing the full length *pcs* cDNA, a 500 bp GFP linker, and the full length *pcs* cDNA cloned in the opposite orientation. This entire insert was then subcloned into pUAST using *Kpn*I and *Xba*I. Upon expression, this transcript double-backs upon itself forming a hairpin double-stranded RNA that can be processed for RNAi (Piccin et al., 2001). Both constructs were injected into *yw* embryos according to published transgenic procedures (Baylies and Bate, 1996).

Generation of Pcs polyclonal antibody

The full length *pcs* cDNA was cloned into pGEX-2T, and Glutathione *S*-transferase (GST) fusion proteins were produced in DH5α *E. coli* using standard induction conditions. GST-Pcs proteins were purified by Glutathione Sepharose beads according to manufacturer's instructions (Amersham Pharmacia Biotech) and concentrated using Centriprep centrifugal filter devices (Millipore). This bacterially expressed and purified GST-Pcs was injected into rabbits at Pocono Rabbit Farm and Laboratory (Canandensis, PA), according to standard protocols. We confirmed antibody specificity by performing Western blots on protein extracts from wild type and pcs^{gs} mutant adults (Supplementary Fig. 1A). As previously described, Pcs protein is detected as a 53–55 kDa doublet (Sinka et al., 2002). This doublet is absent in protein extracts made from adults lacking Pcs expression indicating the specificity of the anti-Pcs antiserum to Pcs protein.

Immunohistochemistry

Immunocytochemistry in embryos was performed as described by Artero et al. (2003), with the following modifications. Antibodies were preabsorbed (PA) against fixed *yw* embryos or in combination with the TSA system (TSA; PerkinElmer Life Sciences). Antibody dilutions were: anti-Mhc (1:10,000; TSA; a gift from D. Kiehart), anti-Kr (1:2000; PA; provided by J. Reinitz), anti-Eve (1:3000; PA), anti-Wg (1:500; PA; Developmental Studies Hybridoma Bank), anti-FasIII (1:100), anti-Twi (1:5000; PA; a gift from S. Roth), anti-Zfh1 (1:5000; provided by Z.C. Lai), anti-β-gal (1:2000; Promega), anti-Osk (1:12,000; provided by A. Ephrussi), anti-Lmd (1:1500; PA; provided by H. Nguyen), and anti-Pcs (1:500; PA). Biotinylated secondary antibodies were used in combination with Vector Elite ABC kit (Vector Laboratories, CA). Specimens were embedded in Araldite and images captured using an Axiocam camera (Zeiss) using Adobe Photoshop software. Fluorescent immunocytochemistry using anti-Pcs (1:6000; PA) was detected with the TSA-FITC system (PerkinElmer Life Sciences). Anti-β-gal (1:1000; Promega), anti-CD2 (1:10,000; Serotec), anti-Tec29 (1:10; provided by S. Beckendorf), anti-Twi (1:1000; PA; a gift from S. Roth), and anti-Mhc (1:1000) were detected using Cy3- or FITC-conjugated secondaries and analyzed using a Zeiss LSM510 confocal microscope. *Pcs* RNA localization was detected using digoxigenin-labeled RNA probes, as described (O'Neill and Bier, 1994).

Western blot analysis

Whole adults or bleach-dechorionated embryos were processed in 2× Laemmli's sample buffer (125 mM Tris–HCl, pH 6.8, 20% glycerol, 4% SDS, and Bromophenol blue). Extract equivalents of approximately 3 adults or 10 embryos were loaded per lane on 10% SDS-PAGE gels. Proteins were transferred to PVDF membrane (Amersham Biosciences) at 60 V for 90 min in cold transfer buffer (10 mM CAPS, pH 11, 10% methanol). Benchmark Prestained Protein Ladder (GibcoBRL) was used as a molecular weight marker. Blots were blocked using 5% dry milk in TBST and incubated with anti-Pcs antibody diluted 1:1000 (preabsorbed against yw embryos) and anti-α-tubulin (Accurate Chemical and Scientific Corporation) diluted 1:500 in 5% dry milk in TBST. Membranes were washed in 5% dry milk in TBST and incubated with peroxidase-conjugated anti-rabbit (for Pcs; Sigma) or donkey anti-rat (for α-tubulin; Accurate Chemical and Scientific Corporation) secondary antibodies in 5% dry milk in TBST. Signals were detected with enhanced chemiluminescence (Amersham Biosciences).

Results

Pcs is expressed in the mesoderm and enriched specifically in FCMs

A previous study has described Pcs expression during oogenesis (Sinka et al., 2002). Since our screen suggested a role for Pcs during muscle development, we focused on the embryonic expression pattern of Pcs protein. Immunocytochemistry revealed that Pcs is expressed in the mesoderm throughout embryogenesis (Figs. 1A–C). Pcs protein was detected in the mesoderm at stage 10 as the mesoderm is allocated into different tissues (Fig. 1A). At stage 11, Pcs is strongly expressed in the visceral and somatic mesoderm during FC and FCM specification (Fig. 1B). From stage 12 to the end of embryogenesis, Pcs was expressed at high levels in the somatic mesoderm as myoblasts fuse and muscles achieve their final morphology (Fig. 1C). Pcs expression in the visceral mesoderm diminishes during these stages, and Pcs protein is not detected in the final muscles (data not shown). Expression of *pcs* mRNA in wild type embryos was also analyzed. This expression mirrored that of Pcs protein during the early stages of mesoderm and somatic mesoderm development, except that *pcs* mRNA was detected in the mesoderm slightly earlier, from stage 9 onwards (data not shown).

Our previous microarray and Northern blot analysis focused on *pcs* expression during FC and FCM specification and predicted that *pcs* is particularly enriched in FCMs (Artero et al., 2003). To confirm this prediction, we tested whether *pcs* expression levels correlated with the number of FCMs specified (Figs. 1D–I). First, we analyzed *pcs* expression levels when FCM number was decreased either by decreasing Notch (N) signaling or increasing Ras signaling (Artero et al., 2001; Bour et al., 2000; Carmena et al., 2002). In embryos lacking all zygotic *N* expression, reduced FCM numbers are detected and a corresponding reduction in *pcs* levels was found (Fig. 1E). Likewise, when FCM numbers were reduced by increasing Ras signaling in the mesoderm by overexpressing an activated form of the Ras protein (Ras^{V12}), a decrease in *pcs* mRNA levels in the mesoderm was detected (Fig. 1F). We next increased FCM numbers by activating N signaling (by overexpressing an activated form of the N receptor [N^{intra}]) or by reducing Ras signaling (by overexpressing a dominant negative form of Ras [Ras^{N17}]) in the mesoderm (Artero et al., 2001; Carmena et al., 2002). In both cases, an increase in FCM number was found with a concomitant increase in *pcs* expression levels (Figs. 1G–I). However, increasing N signaling increased *pcs* levels much more than decreasing Ras signaling, suggesting that *pcs* expression may be directly regulated by N signaling in FCMs. Indeed, sequence analysis has identified several potential Suppressor of Hairless (Su(H)) binding sites in the first intron of the *parcas* gene (data not shown). Together, these data

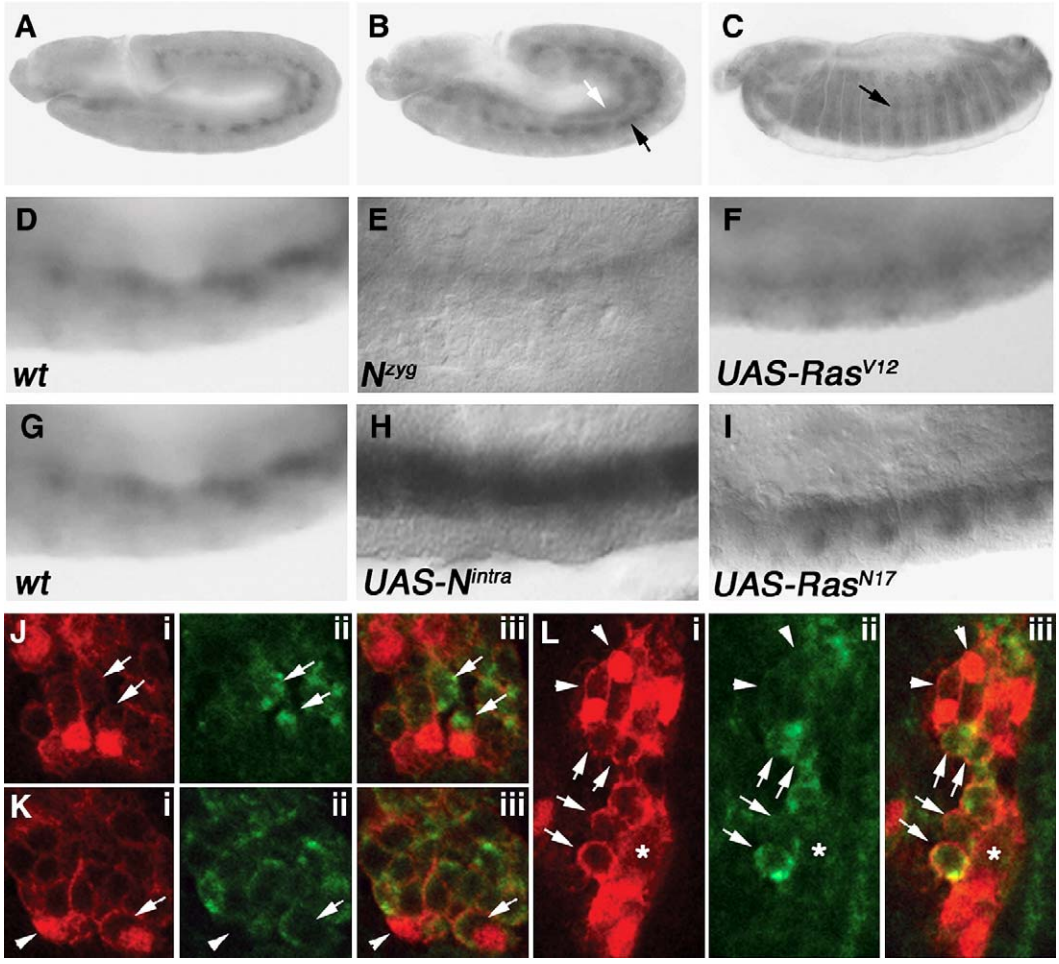

Fig. 1. Pcs is expressed in the developing mesoderm and specifically enriched in FCMs. In all panels, anterior is left and dorsal is up. Staging is according to Campos-Ortega and Hartenstein (1985) in all figures. (A) At stage 10, Pcs is expressed throughout the mesoderm. This expression continues to stage 11 (B) where it is expressed in the somatic (black arrow), cardiac, and visceral mesoderm (white arrow). (C) Pcs is expressed in the somatic mesoderm throughout myoblast fusion and muscle morphogenesis (black arrow, stage 14). (D–I) *Pcs* expression levels at stage 11 correlate with the number of FCMs specified. (D, G) *Pcs* is expressed at moderate levels in the mesoderm at stage 11. (E, I) Decreasing the number of FCMs specified by using an *N* mutant embryo (E) or expressing an activated form of the Ras protein (*UAS-Ras*^{V12}) throughout the mesoderm (I) causes a decrease in *pcs* levels. Increasing the number of FCMs specified by expressing a constitutively activated form of the N receptor (*UAS-N*^{intra}; F) or a dominant negative form of Ras (*UAS-Ras*^{N17}; H) causes an increase in *pcs* levels. (J–L) Pcs is enriched in FCMs. The panels shown are close-ups of the ventral–lateral somatic mesoderm. Anti-Pcs (green), anti-β-Gal (red nuclear), and anti-CD2 (red membrane) staining and merges are shown in stage 12 (J, K) and stage 14 (L) *rP298; twi-CD2* embryos. The enhancer trap insertion rP298 marks FCs in somatic and visceral mesoderm (Ruiz-Gomez et al., 2000). Twi-CD2 labels the plasma membrane of all FCs and FCMs (Borkowski et al., 1995). Panels J and K show two optical sections from a single z-stack. Panel J shows the most external layer of mesodermal cells, while panel K is more interior. Pcs is expressed in FCMs surrounding FCs (white arrows, J). However, low levels of Pcs expression are observed in a single ventral FC (white arrow, K) and lateral FC (data not shown). Pcs expression is absent from all other FCs at this stage (white arrowhead, K). (L) Pcs is enriched in FCMs throughout the fusion process. At stage 14, Pcs is enriched in FCMs (white arrows, L) and completely absent from growing myotubes (white arrowheads, L). Pcs expressing FCMs can be observed lining up alongside the myotube that will form muscle VA1 (white asterisk, L).

indicated that *pcs* expression in the mesoderm at the time of FC and FCM specification correlated with the numbers of FCMs specified. These data supported the prediction that *pcs* is enriched in FCMs at this stage of development.

To further examine the FCM expression and cellular localization of Pcs, we analyzed Pcs expression in the mesoderm using fluorescent immunocytochemistry. We performed these experiments in embryos expressing *rP298*, which is a lacZ-containing P element insertion into the *dumbfounded* (*duf*) gene and labels the nuclei of all FCs (Ruiz-Gomez et al., 2000), and a mesodermal reporter gene (*twi-CD2*), which labels the membranes of all FCs and FCMs (Borkowski et al., 1995). These *rP298; twi-CD2* embryos were simultaneously labeled with antibodies to β-galactosidase, CD2, and Pcs. In these embryos, we identified FCs by the expression of rP298 and twi-CD2 and all FCMs by expression of twi-CD2 and lack of rP298. We detected low levels of Pcs expression throughout the somatic mesoderm at stage 11 (data not shown). However, by stage 12, Pcs expression is strongly upregulated in all FCMs (Figs. 1J, K). Pcs expression was also observed at low levels in a single ventral (Fig. 1K) and lateral (data not shown) FC at this stage of development. However, we have been unable to determine the identity of these FCs using available markers. This limited FC expression is transient as no Pcs expression was observed in growing myotubes (Fig. 1L). As myoblast fusions proceed, Pcs expression is maintained at high levels in all FCMs

(Fig. 1L). Pcs was specifically excluded from the nucleus and was enriched in the cytoplasm and at the cell membranes of FCMs (Figs. 1J–L). These data indicated that Pcs is expressed throughout the somatic mesoderm at the time of mesodermal patterning and FC specification, while later during muscle morphogenesis it is specifically expressed in FCMs.

Embryos lacking all maternal and zygotic expression of pcs show defects in mesodermal patterning, muscle specification and muscle morphogenesis

The specific expression of Pcs during several distinct periods of mesoderm and somatic muscle development implied that *pcs* may play important roles in regulating these processes. We tested this hypothesis first by analyzing muscle development in embryos lacking all *pcs* expression. Flies homozygous for a null allele of *pcs* (pcs^{gs}) are adult viable with reduced egg-laying capacity. We therefore collected embryos laid by *pcs* homozygous mutant females crossed to *pcs* homozygous mutant males. These embryos lacked all maternal and zygotic expression of *pcs* and are referred to as pcs^{gs} *m+z* embryos.

Wild type embryos have a segmentally repeated, distinct array of 30 muscles per hemisegment (Figs. 2A, C and 6A, D, G). In pcs^{gs} *m+z* embryos, one third of these embryos show a severe muscle phenotype including the absence of many muscles, large numbers of unfused myoblasts present often where a missing muscle should be located, and defects in muscle morphology ($n=32$). Muscles, although specified, were often not the correct size, shape, and orientation and attached incorrectly to the overlaying epidermis (Figs. 2B, D and 6B, E, H). In addition, we observed that the posterior segments were most often affected (Fig. 6H). The severity of these muscle defects is variable. While one third of embryos show a severe muscle phenotype, the remaining embryos display only mild to moderate defects in the final muscle pattern. This variability is true for all the phenotypes described below. In addition, only 60% of moderately to severely affected embryos ($n=27$) displayed a large number of unfused myoblasts. These unfused myoblasts are predominantly in segments lacking many muscles (data not shown). Given these phenotypes and the mesodermal expression of Pcs described above, we hypothesized that *pcs* may be required for normal muscle development to occur. We therefore analyzed earlier steps of muscle development in these mutant embryos to determine the cause of these muscle phenotypes and correlate these defects with Pcs expression.

A likely explanation for the observed increase in unfused myoblasts, particularly in the light of the observed missing muscles, was that FCs were not being correctly specified, leading to FCMs with no FC with which to fuse. Thus, two FC markers, Even-skipped (Eve) and Krüppel (Kr), were used to analyze FC specification in pcs^{gs} *m+z* mutant embryos. In wild type embryos, Eve is expressed in a discrete cluster of cells in the dorsal mesoderm of each hemisegment that will form the dorsal DA1 muscle and two pericardial cells (Fig. 2E) (Carmena et al., 1998). In pcs^{gs} *m+z* mutant embryos, we observed frequent disruptions of Eve expression, indicating a loss of Eve-positive FCs (Fig. 2F). This Eve expression loss corresponded with an absence of the Eve-expressing dorsal muscle DA1 (Fig. 6H) and pericardial cells (data not shown) later in development. Kr is normally expressed in a subset of FCs in the dorsal, lateral, and ventral mesoderm (Fig. 2G) (Ruiz-Gomez et al., 1997). However, in pcs^{gs} *m+z* mutant embryos, occasional losses of Kr expressing FCs were observed (Fig. 2H). Together, these data revealed that pcs^{gs} *m+z* mutant embryos have defects in FC specification that most likely account for the muscle losses observed in the final muscle pattern.

Since Pcs is not expressed, for example, in Eve-expressing FCs (data not shown), but is expressed prior to FC specification, we investigated whether these FC losses could be due to an earlier defect in mesodermal patterning. Therefore, we analyzed early mesodermal patterning in pcs^{gs} *m+z* mutant embryos. In wild type embryos, Twist is expressed in all mesodermal cells at high levels at stage 9 (Fig. 2I) and is necessary for mesodermal specification (Thisse et al., 1987). Subsequently, Twist levels are modulated at stage 10, when Twist is required for allocation of mesoderm into its different tissue types (Baylies and Bate, 1996). In pcs^{gs} *m+z* mutant embryos, we observed reduced Twist levels as well as a "twisted" phenotype, reminiscent of the phenotype displayed by *twist* mutant embryos (Fig. 2J) (Thisse et al., 1987). The number of Twist-expressing cells appears to be normal. Given this effect on Twist expression, we also determined if mesodermal tissues other than body wall muscles were affected. Wild type embryos stained with an antibody against Fasciclin III (FasIII) show a stripe of FasIII-positive cells along the A–P axis of the embryo that will eventually form the gut muscles of the embryo (Fig. 2K) (Baylies and Bate, 1996). In pcs^{gs} *m+z* mutant embryos, we observed gaps in FasIII staining, indicating a loss of visceral mesoderm (Fig. 2L). The presence of cardiac mesoderm was assayed using the marker Zinc Finger Homeodomain 1 (Zfh1), which is expressed in four rows of cells, cardioblasts, and pericardial cells, along the dorsal side of the embryo (Fig. 2M) (Lai et al., 1991). In pcs^{gs} *m+z* mutant embryos, Zfh1-positive cells were missing, indicating a loss of cardiac mesoderm (Fig. 2N). Hence, the phenotypic analysis indicated that pcs^{gs} *m+z* mutant embryos show defects at two steps of muscle development. First, these embryos showed defects in early mesodermal patterning. Pcs^{gs} *m+z* mutant embryos showed an early reduction in Twist expression levels (Fig. 2J) and a concomitant decrease in somatic, visceral, and cardiac lineages (Figs. 2B, D, F, H, J, L, N). Second, these embryos show defects in muscle morphogenesis. In the muscles that are specified in pcs^{gs} *m+z* mutant embryos, a number of morphological defects are observed including defects in muscle size, shape, and orientation (Figs. 2B, D and 6A, D, G).

Pcs is required during oogenesis for posterior patterning and segmentation

Although the phenotypic analysis of pcs^{gs} *m+z* mutant embryos suggested that Pcs may play multiple roles in muscle development, we found additional defects in segmentation and

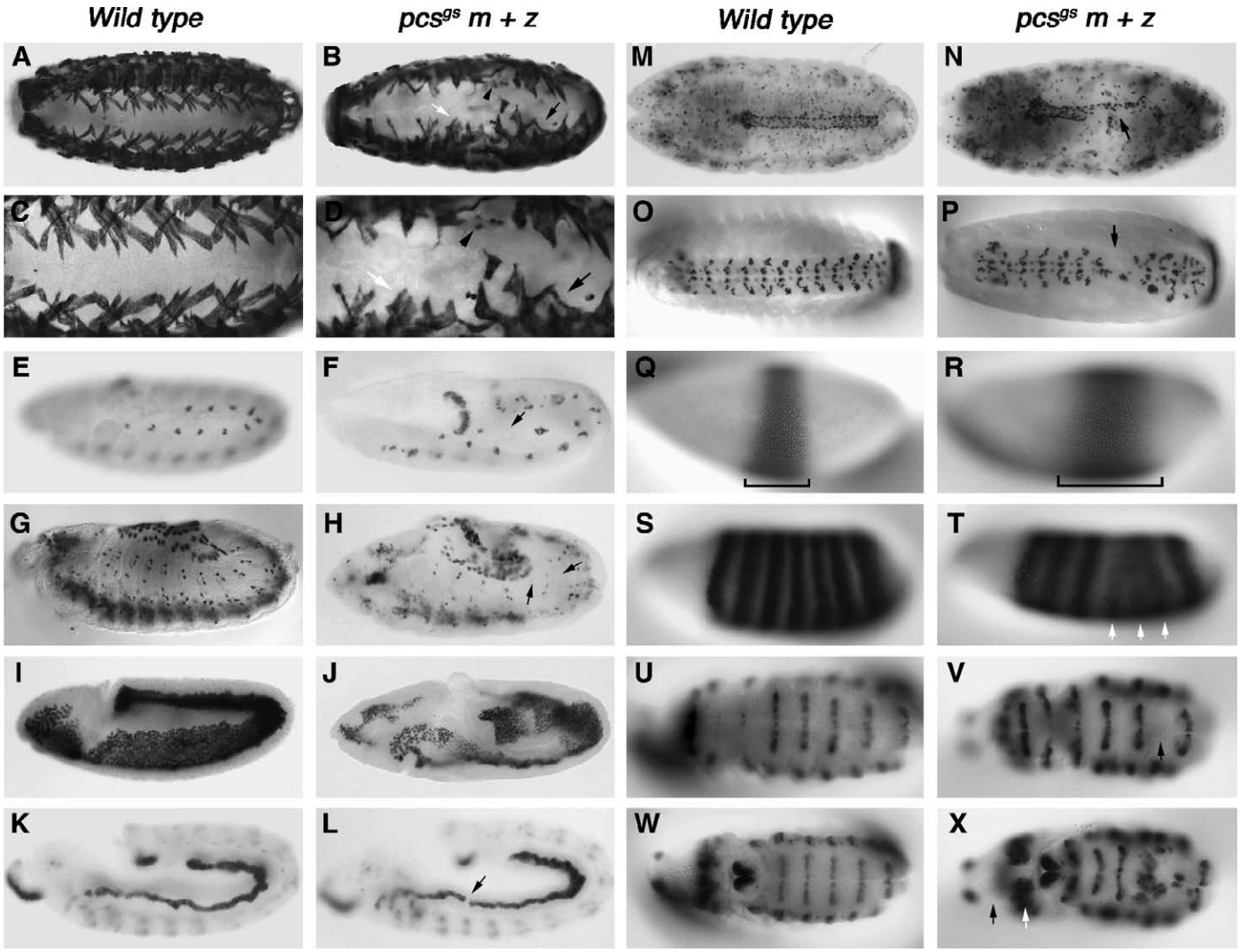

Fig. 2. *Pcs*^{gs} *m+z* mutant embryos display defects in muscle development, mesodermal patterning, segmentation, and early patterning events. Anterior is left and dorsal is up unless otherwise noted. All views are lateral except for panels A–D, O, P, U, and V, which are ventral or panels M, N, W, and X, which are dorsal. Wild type and *pcs*^{gs} *m+z* mutant embryos were stained with antibodies against MHC (A–D), Eve (E, F, O, P, S, T), Kr (G, H, Q, R), Twi (I, J), FasIII (K, L), Zfh1 (M, N), and Wg (U–X). (A–N) *Pcs* is required for the specification and patterning of mesodermal tissues. (A–D) *pcs*^{gs} *m+z* mutant embryos show losses of muscles (black arrow, B, D), unfused myoblasts (black arrowhead, B, D) and defects in muscle morphology (white arrow, B, D). (E–H) *Pcs* is required for FC specification. (E) In stage 11 wild type embryos, Eve is expressed in a subset of FCs in the dorsal mesoderm of each hemisegment. (F) *Pcs*^{gs} *m+z* mutant embryos show losses of Eve expression (black arrow, F). (G) Kr is expressed in a subset of dorsal, lateral, and ventral FCs in stage 12 wild type embryos. (H) Losses of Kr expressing FCs are observed in *pcs*^{gs} *m+z* mutant embryos (black arrows, H). (I–N) *Pcs*^{gs} *m+z* mutant embryos display general mesodermal patterning defects. (I) Twi is expressed at high levels in all mesodermal cells at stage 9 in wild type embryos, while *pcs*^{gs} *m+z* mutant embryos show a reduction in Twi expression levels and aberrant mesodermal patterning (J). (K, L) Losses of visceral mesoderm at stage 11 are also detected in *pcs*^{gs} *m+z* mutant embryos as shown by gaps in FasIII staining (black arrow, L). The embryo shown displays a relatively subtle phenotype with only small gaps in FasIII staining. More severely affected embryos show more dramatic losses of visceral mesoderm. (M, N) *Pcs*^{gs} *m+z* mutant embryos show losses of cardiac mesoderm as indicated by losses of Zfh-1 positive cardioblasts at stage 16 (black arrow, N). (O–X) *Pcs* is required for early patterning and segmentation. (O, P) *Pcs*^{gs} *m+z* mutant embryos show losses of neurons in the CNS as shown by loss of Eve-expressing cells in the ventral nerve cord at stage 16 (black arrow, P). (Q) The gap gene *Kr* expressed a distinct domain in the center of the embryo at blastoderm stages (black bracket, Q). This domain of Kr expression is expanded in *pcs*^{gs} *m+z* mutant embryos (black bracket, R). (S) The pair-rule gene *Eve* is expressed in seven stripes along the A–P axis of the blastoderm embryo. (T) *Pcs*^{gs} *m+z* mutant embryos show losses of Eve expression, specifically within stripes 4, 5, and 6 (white arrows, T). (U, W) In wild type embryos, Wg is expressed in fourteen stripes of cells along the A–P axis. (V, X) *Pcs*^{gs} *m+z* mutant embryos show both losses (black arrows, V, X) and aberrant patterning (white arrow, X) of these Wg stripes.

patterning of other tissues in these embryos. For example, losses of Eve-expressing neurons in the CNS of *pcs*^{gs} *m+z* mutant flies were observed (Fig. 2P) (Doe et al., 1988). This phenotype was unexpected because Pcs expression was not detected in wild type CNS. These data suggested a more general defect in early patterning and segmentation that could account for some of the mesoderm and muscle phenotypes described above. Therefore, we analyzed the expression of several classes of segmentation genes responsible for early embryonic patterning in *pcs*^{gs} *m+z* embryos.

We first analyzed expression of the gap gene *Kr* during segmentation in *pcs*^{gs} *m+z* mutant embryos. In wild type

embryos, Kr has a broad domain of expression in the center of the embryo (Fig. 2Q) (Gaul and Jackle, 1987). This expression domain is established by overlapping gradients of expression of maternal effect genes, such as *nos* and *bicoid* (*bcd*) (Manseau and Schupbach, 1989). In pcs^{gs} *m+z* mutant embryos, however, this expression domain was expanded posteriorly (Fig. 2R). Next, we examined expression of the pair-rule gene *eve*. Eve is expressed in seven stripes along the A–P axis in a wild type embryo during segmentation (Fig. 2S) (Frasch et al., 1987; Macdonald et al., 1986). These stripes of expression are established by overlapping expression of gap genes. In pcs^{gs} *m+z* mutant embryos, reduced levels of Eve expression were observed, specifically in stripes 4, 5, and 6 (Fig. 2T). Finally, expression of the segment polarity genes *wg* and *engrailed* (*en*) was examined. During segmentation, Wg is expressed in fourteen stripes along the A–P axis of the embryo (Figs. 2U, W) (Gonzalez et al., 1991). In pcs^{gs} *m+z* mutants, we observed missing or aberrantly patterned Wg stripes. These losses of Wg stripes are predominantly in the posterior of the embryo, but occasional losses were detected in the most anterior abdominal segments (Figs. 2V, X). These defects in Wg expression were first detected at stage 8 and were maintained throughout subsequent development. In addition, we noted losses of En stripes in pcs^{gs} *m+z* mutant embryos (data not shown). These data confirmed previously published results suggesting that *pcs* is required maternally for posterior patterning in the embryo (Sinka et al., 2002).

The posterior patterning defects observed in pcs^{gs} *m+z* mutant embryos were consistent with those predicted to be caused by a reduction of Osk levels at the posterior pole of the embryo. Indeed, Sinka et al. (2002) observed a reduction in Osk levels in pcs^{gs} mutant embryos. As Osk localization at the posterior pole is established during oogenesis (Ephrussi et al., 1991), we next determined whether all aspects of the posterior patterning defects observed in pcs^{gs} *m+z* mutant embryos were due to a maternal requirement for *pcs*. We thus collected pcs^{gs} *mat* embryos, which lack all maternal expression of *pcs*, but express *pcs* zygotically (Fig. 3). When posterior patterning in pcs^{gs} *mat* embryos was analyzed by examining expression of the gap gene *Kr*, we observed similar phenotypes to those seen in pcs^{gs} *m+z* mutant embryos, namely an expansion in Kr expression towards the posterior of the embryo (Fig. 3E). We found the same defects described for pcs^{gs} *m+z* mutant embryos for expression of the pair-rule gene *eve* (Fig. 3H) and the segment polarity gene *wg* (Fig. 3K). These data indicated that the posterior patterning defects described above are due specifically to a requirement for *pcs* during oogenesis.

Loss of pcs during oogenesis causes global defects in mesodermal patterning

We next addressed what aspects of the muscle defects described above were also due to a maternal requirement for *pcs*. We first analyzed early mesodermal patterning by looking at Twi expression. In pcs^{gs} *mat* mutant embryos, we observed a reduction in Twi expression levels and a "twisting" phenotype identical to that observed in pcs^{gs} *m+z* mutant embryos (compare Figs. 2J and 3N). This indicated that the defects in early mesodermal patterning described above were due to the loss of maternal Pcs expression. We next analyzed the final muscle pattern. In pcs^{gs} *mat* mutant embryos, we observed incompletely penetrant and variable defects in the final muscle pattern. 37% of embryos showed a moderate to severe phenotype (Figs. 3Q, T, $n=19$) with the remaining mutant embryos showing mild to moderate defects. Muscle defects observed include muscle losses, unfused myoblasts, and defects in muscle morphology. The posterior segments were most severely affected, but curiously, anterior segments also displayed the same classes of patterning defects.

We next asked whether the observed global loss of mesodermal patterning is caused by the defects in posterior patterning described above. There are two Osk protein isoforms expressed in the oocyte, a short 55 kDa isoform and a long 71 kDa isoform (Markussen et al., 1995). Western blot analysis of pcs^{gs} mutant ovaries showed a significant reduction in levels of the short Osk isoform, while levels of the long Osk isoform were unaffected (Sinka et al., 2002). Previous studies have indicated that the short Osk isoform is necessary and sufficient to induce the formation of abdomen and germline within the embryo (Markussen et al., 1995). We therefore determined what effects specifically removing the short Osk isoform would have on both embryonic patterning and muscle development. To do this, we expressed a transgene encoding the long Osk isoform (*oskM139L*) in osk^{54}/Df females, which express no Osk protein, and crossed them to *yw* males. The only Osk protein expressed in the ovaries and oocytes of those females is the long isoform. Embryos laid by *oskM139L;* osk^{54}/Df females show a reduction in Osk levels as previously described (Fig. 3C) (Markussen et al., 1995).

When we analyzed embryonic patterning in embryos laid by females only expressing the long Osk isoform, we saw identical classes of phenotypes to those observed in embryos laid by pcs^{gs} mutant females. However, in all cases, the defects in *oskM139;* osk^{54}/Df *mat* embryos were more severe than those observed in pcs^{gs} *mat* embryos. Kr expression was expanded towards the posterior of the embryo (Fig. 3F), and a complete loss of Eve expression in stripes 4, 5, and 6 was observed (Fig. 3I). We also observed losses of Wg expression (Fig. 3L). However, analysis of these embryos was complicated by the "twisting" phenotype observed. This is similar to that observed in the pcs^{gs} *m+z* and pcs^{gs} *mat* mutant embryos described above and suggested a defect in Twi expression or mesodermal specification. Indeed, when we analyzed Twi expression, we observed a reduction in Twi levels, but not number of cells (Fig. 3O). We also observed severe defects in the final muscles in these embryos (Figs. 3R, U). There is a dramatic reduction in the number of muscles, a large number of unfused myoblasts, and defects in muscle morphology. The defects in embryonic patterning and muscle development observed in embryos laid by females

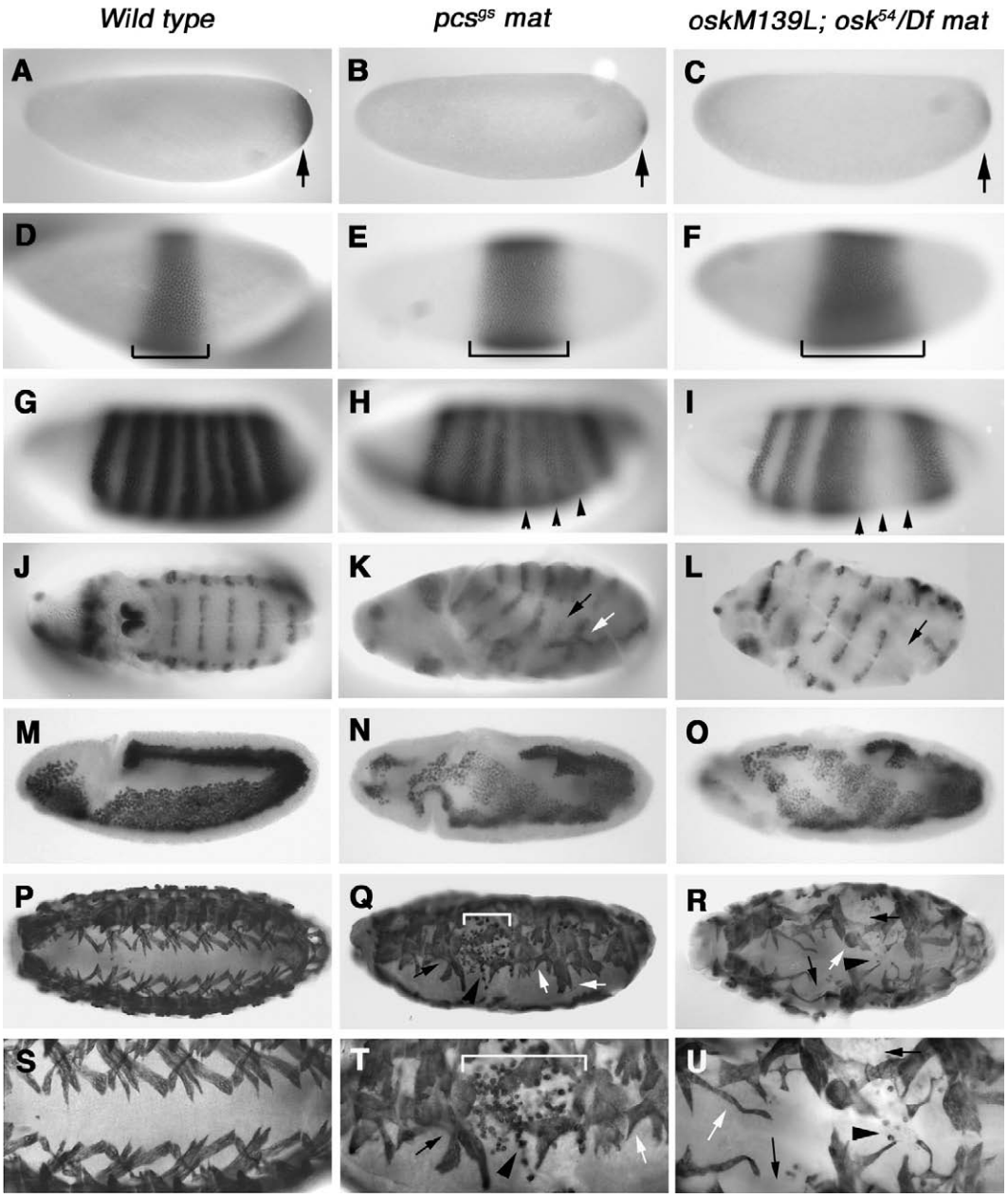

Fig. 3. The *pcs*^{gs} *mat* early patterning and muscle phenotypes are Osk-dependent. Wild type (A, D, G, J, M, P, S), *pcs*^{gs} *mat* (B, E, H, K, N, Q, T), and *oskM139L; osk*^{54}*/Df mat* (C, F, I, L, O, R, U) mutant embryos were stained with anti-Osk (A–C), anti-Kr (D–F), anti-Eve (G–I), anti-Wg (J–L), anti-Twist (M–O), and anti-MHC (P–U). All views are lateral except J–L, P–U which are ventral. (A) Osk protein is tightly localized to the posterior pole in wild type embryos (black arrow). (B) *Pcs*^{gs} *mat* mutant embryos show decreased levels of Osk protein at the posterior pole (black arrow). (C) *OskM139L; osk*^{54}*/Df mat* mutant embryos show lower levels of Osk protein than wild type (A) or *pcs*^{gs} *mat* (B) embryos. (D, E) The Kr expression domain is expanded in *pcs*^{gs} *mat* mutant embryos (black bracket, E) compared to wild type (black bracket, D). (F) Kr expression is expanded in *oskM139L; osk*^{54}*/Df mat* mutant embryos (black bracket, F) more than observed in *pcs*^{gs} *mat* mutant embryos (E). (G) Eve is expressed in seven stripes along the A–P axis in wild type embryos. (H, I) Losses of Eve expression are observed in both *pcs*^{gs} *mat* (black arrows, H) and *oskM139L; osk*^{54}*/Df mat* (black arrows, I) mutant embryos. (J, K) *Pcs*^{gs} *mat* mutant embryos show losses of Wg stripes (black arrow, K) and aberrant patterning of remaining stripes (white arrow, K) compared to wild type (J). (L) *oskM139L; osk*^{54}*/Df mat* mutant embryos show losses of Wg expression (black arrow, L). (M) Twist is expressed at high levels in all mesodermal cells at stage 9. (N, O) Twist levels are reduced in *pcs*^{gs} *mat* (N) and *oskM139L; osk*^{54}*/Df mat* mutant embryos (O). (P, S) Wild type embryos display a segmentally repeated pattern of ventral muscles. (Q, T) *Pcs*^{gs} *mat* mutant embryos show general muscle patterning defects including missing muscles (black arrows, Q, T), unfused myoblasts (black arrowhead, Q, T), and muscle morphology problems (white arrows, Q, T). In addition these embryos display segment-specific defects (white bracket, Q, T). (R, U) *oskM139L; osk*^{54}*/Df mat* mutant embryos show severe defects in muscle development. Large numbers of muscles are missing (black arrows, R, U), and unfused myoblasts are observed (black arrowhead, R, U). Defects in muscle morphology are also observed (white arrows, R, U).

lacking the short isoform of Osk and those laid by females lacking Pcs expression were strikingly similar. Taken altogether, these data strongly suggested that the early patterning and muscle defects observed in *pcs*^{gs} *mat* embryos were primarily due to a reduction in the levels of the short Osk isoform.

Loss of Wg signaling causes segment-specific defects in patterning

In addition to the global mesodermal patterning defects observed in the *pcs*^{gs} *mat* mutant embryos, we observed segment-specific problems: one segment often had a more severe muscle phenotype than its adjacent segments. This severe phenotype included a dramatic loss of muscles and a large number of unfused myoblasts (Figs. 3N, Q). A possible explanation for these segment-specific defects could be effects on Wg expression described above. Much work has highlighted the requirement for Wg signaling from the ectoderm to pattern the mesoderm at multiple times during muscle development (Bate and Rushton, 1993; Baylies et al., 1995; Carmena et al., 1998; Cox and Baylies, 2005; Cox et al., 2005; Halfon et al., 2000; Knirr and Frasch, 2001; Ranganayakulu et al., 1996; Wu et al., 1995). One would therefore predict that loss of Wg signaling within a segment would cause loss of Wg-dependent cell types within that same segment. We thus analyzed the specification of Wg-dependent cell types—founder cells (FCs) and neurons—in *pcs*^{gs} *mat* mutant embryos (Carmena et al., 1998; Doe et al., 1988). Losses of both cell types were found in a segment-specific manner: when Eve-positive FCs were absent, so were the Wg-dependent Eve-positive cells in the CNS in the same segment (data not shown). Next, we correlated the losses of Eve-positive FCs with loss of Wg expression in the same segment. Eve-positive FCs arise in the dorsal mesoderm of each hemisegment at stage 11. At this time, Wg is expressed in a cluster of dorsal ectodermal cells directly overlaying the Eve-expressing cluster (Fig. 4A). In *pcs*^{gs} *mat* mutant embryos, we observed a correlation between Wg loss in the dorsal ectoderm and Eve-positive FCs loss in the dorsal mesoderm of that same segment (Fig. 4B).

Although these results supported our hypothesis that the segment-specific phenotypes observed in the muscle pattern of *pcs*^{gs} *mat* mutant embryos were due to loss of Wg signaling, it did not confirm that the loss of Wg expression observed was directly responsible for the mesodermal phenotypes detected. To test this, we abolished Wg signaling in a segment-specific manner and determined if this reproduced the segment-specific phenotype observed in the final muscle pattern. Embryos expressing dnTCF driven by *prd-GAL4* showed a roughly 50% reduction in Wg levels in *prd*-expressing segments in the ectoderm of stage 11 embryos (Materials and methods; Fig. 4D) When we analyzed the specification of Wg-dependent cell types in the mesoderm, a reduction in the number of Eve-positive FCs was found in *prd*-expressing segments (Fig. 4F). This could be due to either the reduction in Wg expression levels observed in the ectoderm of the embryos or a direct repression of the Wg target gene *eve* by dnTCF expression in the mesoderm (Halfon et al., 2000; Knirr and Frasch, 2001). Finally, we analyzed the final muscle pattern in these embryos; we observed the same segment-specific phenotype as described above (Figs. 4H, J). This phenotype, however, was not as severe as that observed in *pcs*^{gs} *mat* mutant embryos (Figs. 3N, Q). This nevertheless supported our hypothesis that loss of Wg signaling within the segment contributed to the segment-specific defects observed in *pcs*^{gs} *mat* mutant embryos. Hence, Wg is required in a segment-specific manner to specify Wg-dependent cell types in the mesoderm and other tissues.

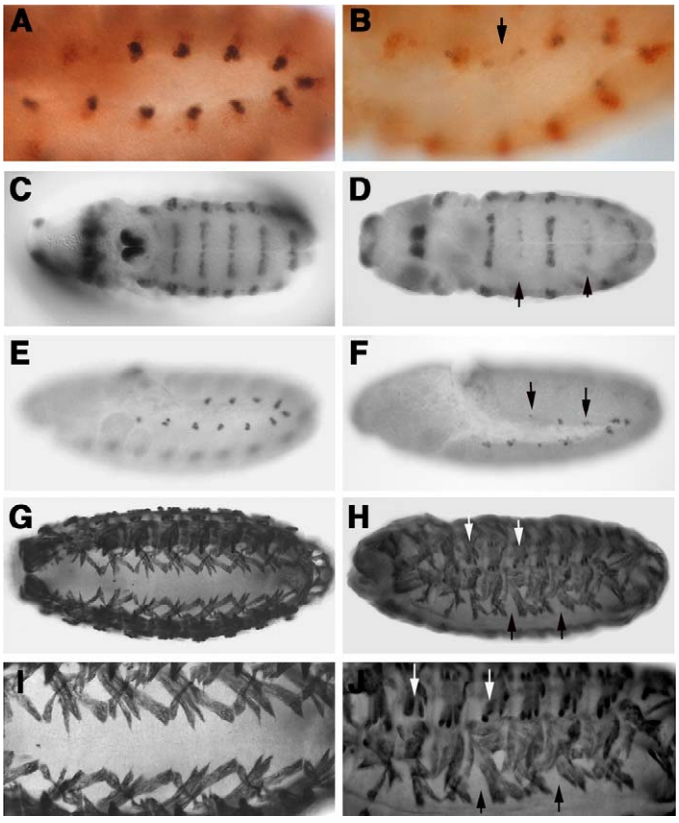

Fig. 4. The segment-specific defects observed in *pcs*^{gs} *mat* mutant embryos are due to loss of Wg expression within that segment. Wild type (A, C, E, G, I), *pcs*^{gs} *mat* mutant (B), and *prd-GAL4>UAS-dnTCF* (D, F, H, J) embryos were stained with anti-Wg (A–D), anti-Eve (A, B, E, F), or anti-MHC (G–J). Lateral views are shown except for C, D, G, I, which are ventral. (A) Wild type embryos show Wg expression in the dorsal epidermis (brown staining, A) directly overlying the Wg-dependent Eve-expressing FCs in the dorsal mesoderm (black staining, A) of each hemisegment at stage 11. (B) In *pcs*^{gs} *mat* mutant embryos, loss of Wg expression in the epidermis corresponds to reduction in Eve expression in the mesoderm of the same hemisegment (black arrow, B). (C) Wild type embryos show normal Wg expression at stage 11. (D) *prd-GAL4>UAS-dnTCF* embryos show reductions in Wg expression levels in *prd*-expressing segments (black arrows, D). (E) Eve is expressed in a subset of Wg-dependent FCs in the dorsal mesoderm of each hemisegment in wild type embryos. (F) Losses of Eve expression are observed in *prd*-expressing segments in *prd-GAL4>UAS-dnTCF* embryos (black arrows, F). (G, I) Wild type ventral muscle pattern at stage 16. (H, J) *prd-GAL4>UAS-dcTCF* embryos show specific muscle defects in *prd*-expressing segments. These defects include loss of Wg-dependent muscles (black arrows, H, J) and muscle morphology defects, especially in the lateral LT muscles, which appear shorter than usual (white arrows, H, J).

Correct levels of Pcs expression are required zygotically for muscle development

While some of the muscle phenotypes observed in *pcs*^{gs} *m+z* mutant embryos are due to a requirement for *pcs* during oogenesis, Pcs expression during muscle development

suggested an additional, zygotic, role for *pcs* during muscle development. We therefore asked whether *pcs* is required zygotically for muscle development by analyzing embryos lacking zygotic expression of *pcs* but that have the maternal contribution of *pcs*. These embryos have normal posterior patterning, and we referred to them as pcs^{gs} *zyg* mutant embryos.

We found reproducible muscle defects, including missing muscles. For example, we observed losses of VO6, VL3, and DA1 muscles in some embryos (Figs. 6C, F, I). We also observed errors in muscle morphology in pcs^{gs} *zyg* mutant embryos. Muscles are often not the correct size, shape, or orientation and attach incorrectly to the overlaying ectoderm (Figs. 5J, N and 6C, F). For example, muscle DT1 often attaches more anteriorly than it should (Fig. 6F). Losses of Eve-expressing FCs (Fig. 5B) were found, corresponding to the missing DA1 muscles observed (Fig. 6I), indicating that *pcs* zygotic activity is required for FC specification and that this may account for the muscle losses observed in the final muscle pattern. As Pcs is not expressed in the Eve-expressing FCs (data not shown), we hypothesized that these FC losses were due to the loss of Pcs expression prior to FC specification. We therefore analyzed early mesodermal patterning in these embryos. However, Twist expression, the earliest marker for mesoderm, was wild type in pcs^{gs} *zyg* mutant embryos, indicating that the mesoderm appeared to be specified and patterned correctly (data not shown). In support of this observation, visceral and cardiac mesoderm formation in these mutant embryos appeared normal (data not shown). Hence, Pcs could be acting on an early mesodermal regulator other than Twist or affecting Twist expression or activity in a way not detected by this assay.

Pcs is specifically enriched in FCMs during muscle morphogenesis. We therefore analyzed FCM specification and differentiation by using an antibody against the FCM-specific protein Lameduck (Lmd, also known as Myoblasts incompetent or Gleeful) (Duan et al., 2001; Furlong et al., 2001; Ruiz-Gomez et al., 2002). However, in pcs^{gs} *zyg* mutant embryos, no defects in Lmd expression were observed (Fig. 5F), suggesting that FCM specification and differentiation occur normally. Together, these data indicated that *pcs* is required zygotically both for muscle specification and morphogenesis.

To confirm that Pcs is required specifically within the mesoderm to establish the correct larval muscle pattern, we

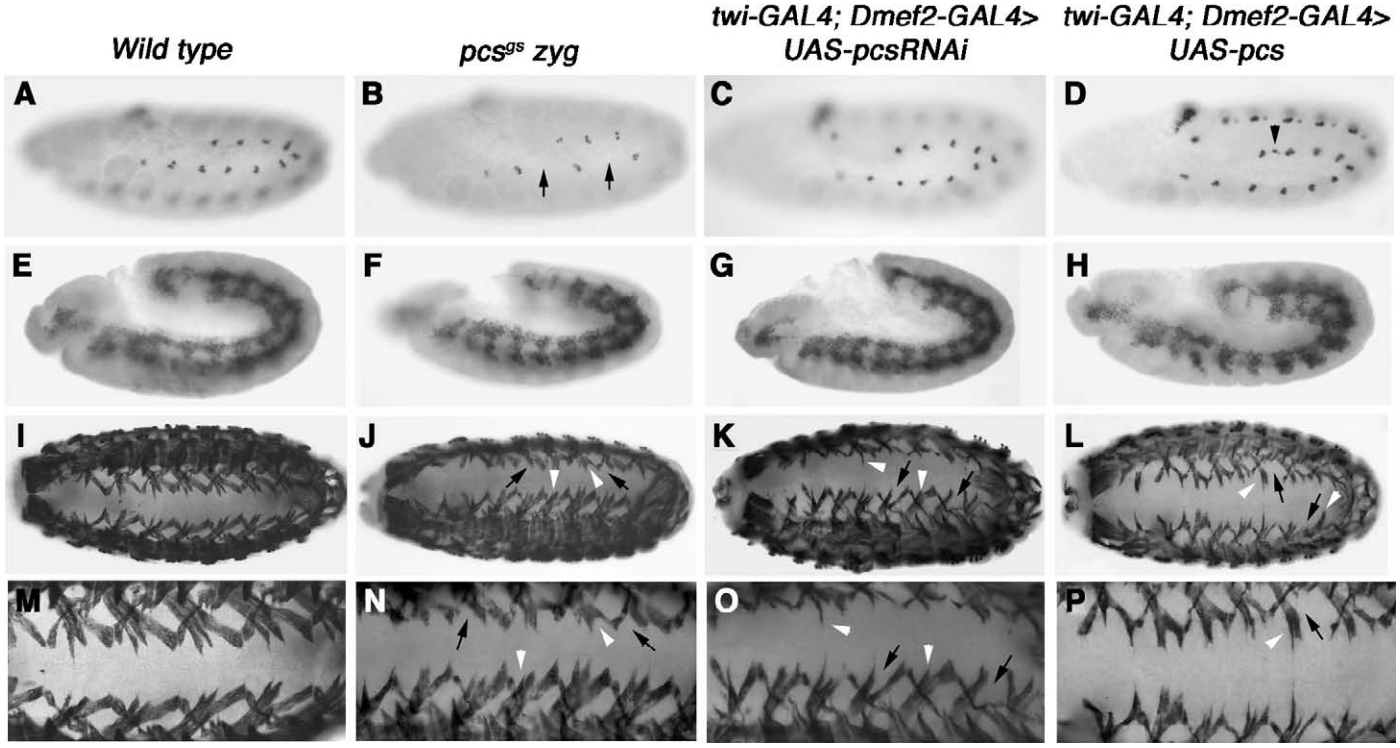

Fig. 5. Correct levels of Pcs are required within the mesoderm for muscle specification and morphogenesis. Wild type (A, E, I, M), pcs^{gs} *zyg* mutant (B, F, J, N), *twi-GAL4; Dmef2-GAL4>UAS-pcsRNAi* (C, G, K, O), and *twi-GAL4; Dmef2-GAL4>UAS-pcs* (D, H, L, P) embryos were stained with anti-Eve (A–D), anti-Lmd (E–H), or anti-MHC (I–P). Panels A–D are lateral views of stage 11 embryos. Panels E–H are lateral views of stage 12 embryos. Panels I–P are ventral views of stage 16 embryos. Panels M–P are close-up views of the embryos shown in panels I–L. (A–D) *Pcs* is required for FC specification. (A) The FC marker Eve is expressed in a subset of FCs in the dorsal mesoderm of each hemisegment in wild type embryos. (B) Pcs^{gs} *zyg* mutant embryos show losses of Eve expression (black arrows, B). (C) Eve expression in *twi-GAL4; Dmef2-GAL4>UAS-pcsRNAi* embryos appears wild type. (D) *twi-GAL4; Dmef2-GAL4>UAS-pcs* embryos show ectopic Eve expression between clusters (black arrowhead, D) and enlarged Eve clusters (data not shown). (E–H) Pcs is not required for FCM specification. (E) Wild type embryos show large numbers of FCMs in each hemisegment. No defects in FCM specification are observed in pcs^{gs} *zyg* (F), *twi-GAL4; Dmef2-GAL4>UAS-pcsRNAi* (G) or *twi-GAL4; Dmef2-GAL4>UAS-pcs* (H) embryos. (I–P) *Pcs* is required for muscle specification and morphogenesis. (I, M) Wild type embryos show a segmentally repeated ventral muscle pattern. Pcs^{gs} *zyg* mutant (J, N), *twi-GAL4; Dmef2-GAL4>UAS-pcsRNAi* (K, O) and *twi-GAL4; Dmef2-GAL4>UAS-pcs* (L, P) embryos all show both losses of muscles (black arrows, J–L, N–P) and defects in muscle morphology (white arrowheads, J–L, N–P).

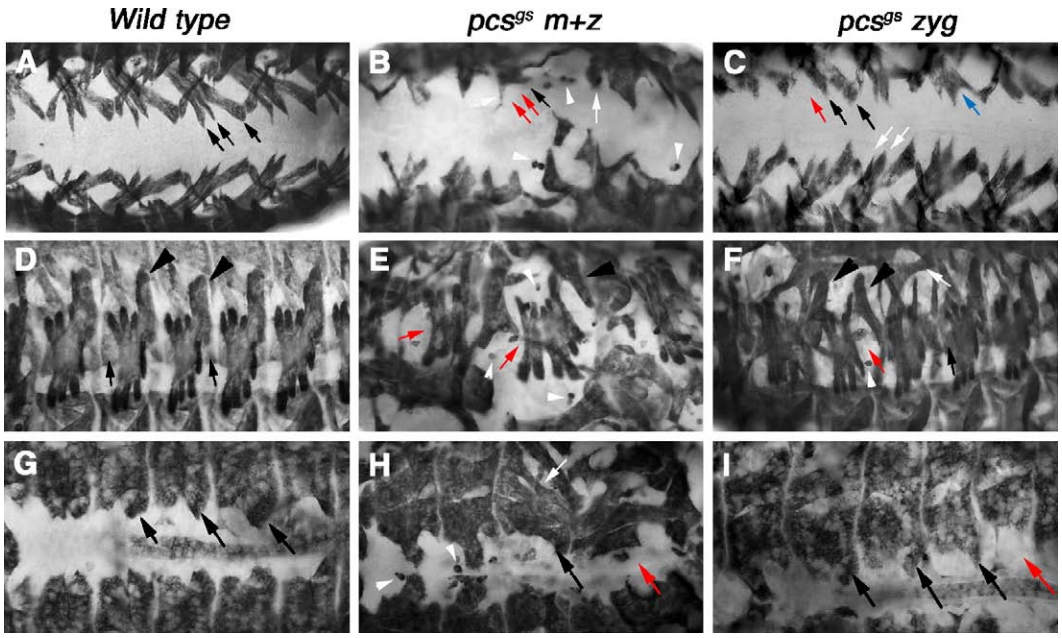

Fig. 6. Pcs is required maternally for global embryonic patterning and zygotically for muscle specification and morphogenesis. Wild type (A, D, G), pcs^{gs} *m+z* (B, E, H), and pcs^{gs} *zyg* (C, F, I) embryos were stained with an antibody against MHC. Ventral (A–C), lateral (D–F), and dorsal (G–I) views of stage 16 embryos are shown. (A, D, G) Wild type embryos show a segmentally repeated pattern of muscles. (A) The ventral muscles VO4, VO5, and VO6 point towards the posterior of the embryo (black arrows, A). (D) Muscles VL1, VL2, VL3, and VL4 span the hemisegment in wild type embryos (black arrows, D), while muscle DT1 runs transverse (black arrowheads, D). (G) Muscle DA1 spans the hemisegment at an acute angle (black arrows, G). (B, E, H) Pcs^{gs} *m+z* show global defects in the final muscle pattern. Specific defects observed include muscle losses (red arrows, B, E), unfused myoblasts (white arrowheads, B, E, H), and defects in muscle morphology (white arrows, B, H). A large number of unfused myoblasts are observed (white arrowheads, B, E, H). (C, F, I) Pcs^{gs} *zyg* mutant embryos show defects in the final muscle pattern. These defects vary between hemisegments and embryos, but include defects in muscle specification and morphogenesis. For example, losses of VO6 (red arrow, C), VL3 (red arrow, F), and DA1 (red arrow, I) muscles can be observed. In addition, muscles are often too small (white arrows, C, F) or the incorrect shape (blue arrow, C). In some cases, muscle attachment appears aberrant. For example, muscle DT1 often attaches more anteriorly than it should (black arrowheads, F). Occasional unfused myoblasts are also seen (white arrowhead, F).

analyzed embryos in which *pcs* expression was specifically removed in the mesoderm by using RNAi (Piccin et al., 2001). A *pcs* RNAi transgene (Materials and methods) was expressed throughout the mesoderm at high levels using *twi-GAL4; Dmef2-GAL4* drivers. We observed a 50% decrease in Pcs expression levels in the *UAS-pcsRNAi* expressing embryos compared to wild type, indicating that our *UAS-pcsRNAi* transgene reduces Pcs levels in vivo (Supplementary Fig. 1B). When the final muscle pattern was examined in these embryos, we found a similar phenotype to that observed in pcs^{gs} *zyg* mutant embryos. Muscle losses and defects in muscle morphogenesis were observed (Figs. 5K, O), but FC (Fig. 5C) and FCM (Fig. 5G) specification occurred normally. We suggest that this discrepancy in the FC specification results is due to the delay in the GAL4/UAS (Brand and Perrimon, 1993) and RNAi (Piccin et al., 2001) systems; hence, sufficient Pcs protein was present prior to the time of FC specification for Eve expression to be normal. Nevertheless, these data confirmed that *pcs* is required specifically within the mesoderm for muscle specification and morphogenesis.

We next asked whether overexpression of Pcs protein would cause defects in muscle development. Analysis of the final muscle pattern in these embryos revealed both muscle losses and defects in muscle morphology. The muscles often appeared thin, and a subset of the ventral muscles approached the midline (Figs. 5L, P). Ectopic expression of Eve was observed between the normally discrete clusters of Eve-expressing FCs in the dorsal mesoderm (Fig. 5D) and occasional expansion of the Eve-expressing clusters was observed (data not shown). However, no defects in Lmd expression were observed (Fig. 5H). Together, these data indicated that correct levels of Pcs are required specifically within the developing mesoderm for both muscle specification and morphogenesis.

Pcs as a regulator of NRTK activity

Pcs is the *Drosophila* orthologue of the mammalian Sab gene, which is known to inhibit the activation of BTK (Matsushita et al., 1998; Yamadori et al., 1999). Previous work has shown that the *pcs* grandchildless phenotype can be suppressed by reducing the maternal dosage of the BTK homologue *Btk29A* (Sinka et al., 2002). We also found that reducing the dose of Btk29A by half was sufficient to observe suppression of the *pcs* grandchildless phenotype (Table 1). We then asked whether reducing the maternal dosage of *Btk29A* by half could suppress the early patterning defects reflected in the loss of the pair-rule Eve and segment polarity Wg expression that were observed in pcs^{gs} *mat* mutant embryos. Under these conditions, we again observed a suppression of the pcs^{gs} *mat* mutant phenotype (Table 1). These results confirmed that Btk29A is a target of Pcs regulation during oogenesis.

Table 1
Effect of reducing *Btk29A* dosage on pcs^{gs} grandchildless, early patterning, and muscle phenotypes

Grandchildless phenotype *			
Maternal genotype	*n*	Wild type	Agametic
pcs^{gs}	109	7%	93%
$Btk29A^{k00206}$, pcs^{gs}/pcs^{gs}	168	26%	74%
**Early patterning (Eve) ** **			
Maternal genotype	*n*	Wild type	Abnormal
pcs^{gs}	13	31%	69%
$Btk29A^{k00206}$, pcs^{gs}/pcs^{gs}	44	50%	50%
**Early patterning (Wg) ** **			
Maternal genotype	*n*	Wild type	Agametic
pcs^{gs}	53	46%	54%
$Btk29A^{k00206}$, pcs^{gs}/pcs^{gs}	40	80%	20%
Muscle development * **			
Parental genotype (F × M)	*n*	Wild type	Abnormal
$pcs^{gs}/CyO \times pcs^{gs}/CyO$	25	92%	8%
$Btk29A^{k00206}$, $pcs^{gs}/CyO \times pcs^{gs}/CyO$	59	85%	15%

* $p<0.001$ for a Chi-squared test.
** $p<0.05$ for a Chi-squared test.
*** $p>0.05$ for a Chi-squared test.

We next addressed if this relationship between Pcs and Btk29A was maintained during muscle development. We first tested if Btk29A was expressed in the mesoderm during embryonic development. We found that Btk29A is expressed in the developing ectoderm, CNS, PNS, and tracheal pits, confirming previous studies (Fig. 7) (Carmena et al., 1995; Katzen et al., 1990; Vincent et al., 1989; Wadsworth et al., 1990). We also observed Btk29A expression in migrating primordial germ cells. Interestingly, Btk29A expression in these cells was localized to the leading edge of the cell (data not shown). Btk29A expression in the developing mesoderm was examined by double staining embryos with Twist antibody (Figs. 7A–F). At stages 10 (Figs. 7A–C) and 11 (Figs. 7D–F), Btk29A expression was detected in a subset of Twist-expressing cells just underneath the overlaying ectoderm. At stage 11, these cells were located adjacent to the developing tracheal pit, where Btk29A is highly expressed (Figs. 7D–F). This mesodermal Btk29A expression then decreased and was absent by stage 13.

We also investigated whether the mesodermal Btk29A expression was in FCs or FCMs. Btk29A expression was analyzed in a genetic background in which all FCs were labeled (*rP298*; Figs. 7G–I). In these embryos, Btk29A was expressed in only one FC at stage 13 (Fig. 7I). This FC was ventral and posterior to the tracheal pit within that segment and did not correspond to the ventral Pcs-expressing FC (data not shown). In addition to expression in a single FC, Btk29A was expressed in a small number of FCMs surrounding it, which also express Pcs. Later in mesodermal development, no muscle expression of Btk29A was found (Figs. 7J–L and data not shown). Taken together, these data indicated that Btk29A is expressed in a subset of mesodermal cells during mesodermal subdivision and FC specification and therefore could potentially be regulated by Pcs at this time. However, these data also demonstrated that Btk29A is not expressed in the majority of Pcs-expressing cells during these stages of somatic muscle development. In addition, Btk29A is not detected in the mesoderm after stage 13 while Pcs is strongly expressed at this time and throughout the remainder of muscle morphogenesis. This suggested that Pcs has additional targets of regulation during muscle development.

To confirm that Btk29A is not the major target of Pcs regulation during muscle development, we tested whether reducing *Btk29A* levels zygotically could suppress the pcs^{gs} *zyg* mutant muscle phenotype. No difference in the penetrance of the muscle specification and morphogenesis phenotypes was observed between pcs^{gs} *zyg* and $Btk29A^{k00206}$, pcs^{gs}/pcs^{gs} *zyg* mutant embryos (Table 1). In addition, we analyzed muscle development in $Btk29A^{k00206}$ homozygous mutant embryos and observed global defects in the final muscle pattern (data not shown). These defects do not correlate with the limited mesodermal expression of Btk29A or with Btk29A being a target of Pcs regulation during oogenesis. We hypothesized that this may be due to the requirement for Btk29A in other tissues such as the epidermis or CNS. To conclude, we have demonstrated that while Btk29A is the major target of Pcs regulation during oogenesis, it does not appear to be an important Pcs target during muscle development.

Discussion

This work highlights the phenomenon of reiterative gene usage by showing that a novel signaling protein, Pcs, is required at multiple times and places during *Drosophila* development. We have confirmed that Pcs is first required during oogenesis to establish anterior–posterior patterning in the developing embryo and that this initial axis determination is required for subsequent development of multiple tissues within the embryo. We also showed that Pcs is required again, specifically within the developing mesoderm of the embryo to regulate both muscle specification and morphogenesis (Fig. 8).

Expression analysis initially identified the tissues where Pcs could play an important role. Previously described studies showed that Pcs is expressed in the ovary and developing oocyte (Sinka et al., 2002). We showed that, in the embryo, Pcs is predominantly expressed in the developing somatic mesoderm throughout muscle development. Pcs is expressed panmesodermally during specification of different mesodermal tissues. Once somatic mesoderm is specified, Pcs expression becomes restricted to the developing somatic muscles where it is maintained throughout the remainder of development. Within the somatic mesoderm itself, we also demonstrated that Pcs is enriched in FCMs as predicted by the microarray screen from which it was isolated (Artero et al., 2003).

Genetic analysis has demonstrated a requirement for *pcs* during oogenesis and muscle development. We have shown that embryos lacking all maternal and zygotic *pcs* expression showed defects both in early patterning and muscle

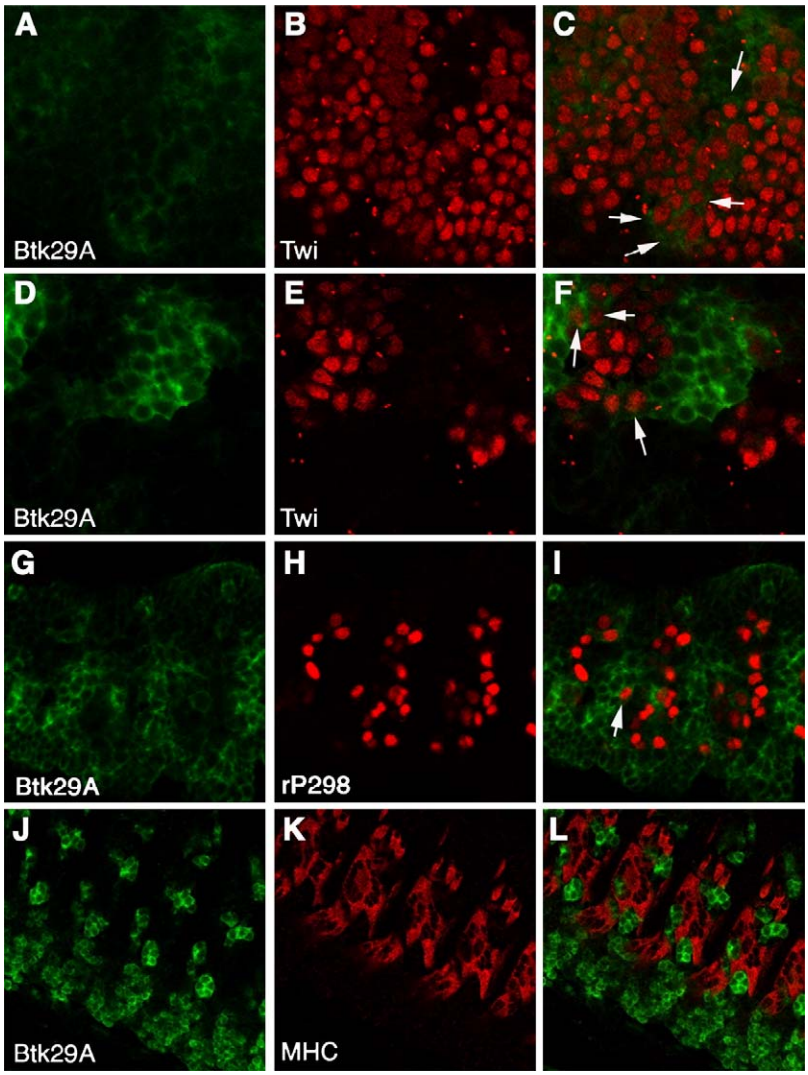

Fig. 7. Btk29A is expressed in a subset of mesodermal cells prior to fusion. Confocal micrographs of wild type (A–F, J–L) and *rP298* (G–I) embryos stained with anti-Btk29A (green, A, D, G, J), anti-Twi (red, B, E), anti-β-gal (red, H), and anti-MHC (red, K). The merged images are shown in C, F, I, and L. Stage 10 (A–C), 11 (D–F), 13 (G–I), and 16 (J–L) embryos are shown. Anterior is to the left and dorsal is up in all panels. (A–C) Btk29A is expressed at low levels in a subset of mesodermal cells (white arrows, C). (D–F) Btk29A expression is maintained in a subset of Twi-positive cells in the somatic mesoderm at stage 11 (white arrows, F). (G–I) Btk29A is then expressed in a single FC (white arrow, I) and surrounding FCMs at stage 13 as fusion begins. (J–L) Btk29A expression in the mesoderm disappears from late stage 13 and is not present in the final muscles at stage 16, even though it is strongly expressed in the CNS and PNS (white arrows, L).

development. Further genetic dissection has demonstrated that *pcs* is required maternally for early patterning and that this requirement for *pcs* can account for some defects observed in the mesoderm and other tissues of the embryo later in development (Fig. 8). We suggest that this maternal requirement for *pcs* is due to its requirement in the ovary. Sinka et al. (2002) showed rescue of the *pcs* grandchildless phenotype by specific expression of *pcs* in the ovary. In addition we examined the zygotic requirement for *pcs* and demonstrated that *pcs* is required specifically in the embryonic mesoderm for both muscle specification and morphogenesis. Therefore, not only is *pcs* required in two different tissues and two distinct times during development, but it is also required multiple times during the development of a specific tissue (Fig. 8). This places Pcs as an important player in multiple developmental processes, yet an important question remains as to how Pcs regulates these distinct processes.

The role of Pcs during oogenesis

One of the most striking results from this work is the demonstration that early patterning defects can cause very specific problems in the subsequent development of multiple tissues. Although gross embryonic patterning defects have been described in the offspring of females carrying mutations in *pcs* and other maternal genes required for early patterning, this has been determined by analyzing the final larval cuticle (Manseau and Schupbach, 1989; Sinka et al., 2002). This is one of the first studies, to our knowledge, that describes the specific defects in patterning of multiple tissues including the body wall muscles, cardiac and visceral mesoderm, CNS, and tracheal system (data not shown) caused by defects in early patterning.

We observed defects in expression of maternal effect, gap, pair-rule, and segmentation genes in pcs^{gs} *mat* mutant embryos, which indicates that the requirement for *pcs* is upstream of these

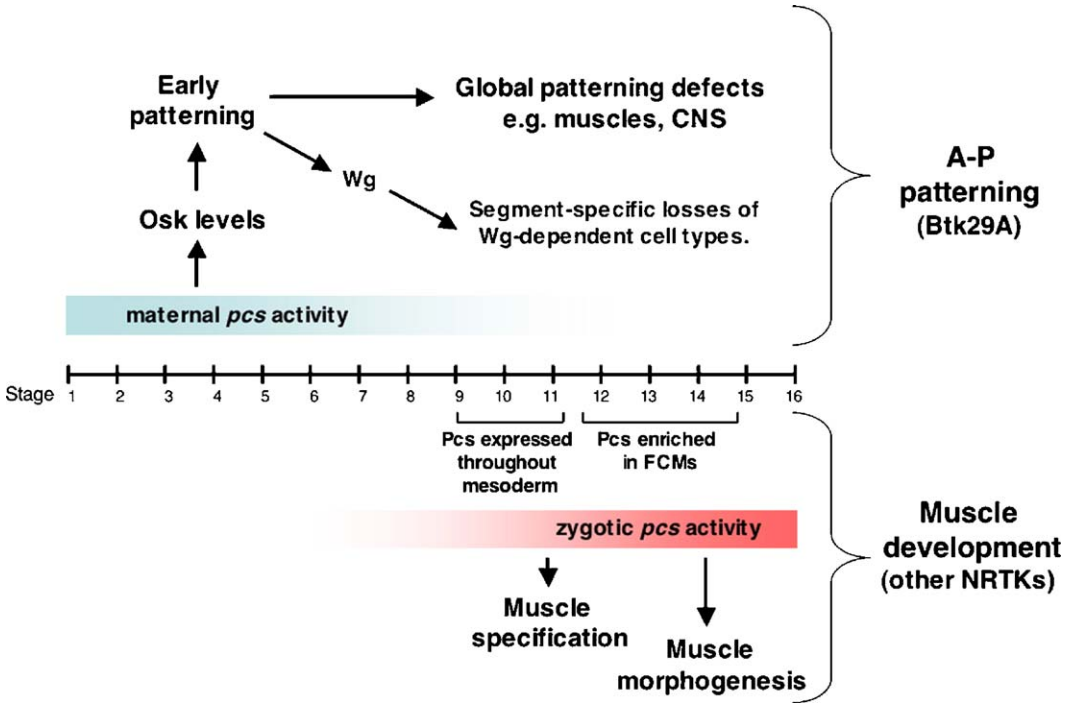

Fig. 8. Pcs function during *Drosophila* development. *Pcs* is required maternally for A–P patterning. A maternal loss of *pcs* activity causes defects in early patterning due to its role in regulating Osk. A subset are due to losses of Wg expression, which cause losses of Wg-dependent cell types in a segment-specific fashion. These early patterning defects cause global patterning defects in the embryo later in development. Genetic data indicate that the major target of maternal Pcs activity is the *Drosophila* Tec kinase Btk29A. *Pcs* is then required zygotically, specifically in the mesoderm, for both muscle specification and morphogenesis. Pcs is expressed throughout the mesoderm prior to its role in muscle specification. It then becomes enriched in FCMs, where we hypothesize that it is required for subsequent muscle morphogenesis. Genetic and expression data suggest that Btk29A is not the major target of zygotic Pcs activity. We propose that Pcs fulfils its zygotic role by regulating the activation of other NRTKs.

factors. This correlates with the previously published work on *pcs*, which showed that *pcs* is required for correct levels of Osk protein at the posterior pole of early embryos (Sinka et al., 2002). We have further shown that specific reduction in levels of the short Osk isoform can reproduce the early patterning and muscle defects observed in pcs^{gs} *mat* mutant embryos. These data strongly suggest that the primary role of Pcs during oogenesis is in regulation of the levels of the short Osk isoform. However, it is formally possible that Pcs could regulate other factors required for early embryonic patterning. The early patterning and muscle defects observed in embryos laid by females only expressing the long Osk isoform are more severe and penetrant than those observed in pcs^{gs} *mat* embryos. In particular, the majority of these embryos do not hatch in contrast to embryos laid by pcs^{gs} mutant females that can survive to adulthood. Previous studies have shown that expression of the short Osk isoform is sufficient to rescue the patterning defects observed in embryos laid by osk^{54}/Df females. These data presented here support that result and go further to show that the small amount of short Osk isoform remaining in pcs^{gs} mutant ovaries is sufficient to partially rescue the osk^{54}/Df phenotype.

The role of Pcs in the mesoderm

The embryonic expression pattern of Pcs and the pcs^{gs} *zyg* mutant phenotype indicated that the major role of Pcs during embryogenesis is in regulating muscle development (Fig. 8). The expression of Pcs in the somatic mesoderm throughout this process suggested that *pcs* is required at multiple steps. This is supported by the phenotypic analysis which demonstrates that *pcs* is required both for muscle specification and morphogenesis. We propose that the loss of Pcs expression during mesodermal patterning and FC specification accounts for the defects in muscle specification, while the loss of Pcs expression in FCMs causes the muscle morphogenesis phenotype observed. This indicated that Pcs is reused at multiple times during the development of this specific germ layer, yet these data also suggested that the Pcs protein itself plays diverse roles. More specifically, Pcs is required both for specifying the fate of a subset of mesodermal cells and for the elaboration of that fate during muscle morphogenesis. Hence, the output of Pcs signaling may depend on context or the target of Pcs regulation (see below).

Detailed analysis of Pcs expression showed an enrichment of Pcs in FCMs as predicted by the microarray screen from which it was identified (Artero et al., 2003). This occurs after FC specification and suggests that the expression of Pcs in FCMs may be required for its role in muscle morphogenesis. Several genes have been shown to be enriched specifically in FCMs and have been demonstrated to be required for myoblast fusion (*sns* and *hbs*) or FCM development (*lame duck/myoblasts incompetent*) (Artero et al., 2001; Bour et al., 2000; Duan et al., 2001; Dworak et al., 2001; Ruiz-Gomez et al., 2002). Some of these genes have also been shown to play a role in muscle

morphogenesis. However, *pcs* is the first FCM-enriched gene demonstrated to be specifically required for this process. This provides further evidence to support the model put forward by Artero et al. (2003) that FCMs make their own contribution to regulating muscle morphogenesis. It also suggests that NRTK signaling is important for this process. To date, NRTK signaling has been shown to be important for the morphogenesis of several tissues in *Drosophila* development (Tsygankov, 2003). These data suggest a possible role for NRTK signaling in muscle development, which needs further investigation.

Pcs as a regulator of NRTK signaling

Pcs is the *Drosophila* orthologue of the mammalian Sab gene. Sab has been shown in vitro and in cell culture to bind and inhibit the activation of the BTK, the *Drosophila* homologue of which is Btk29A (Matsushita et al., 1998; Yamadori et al., 1999). A previous study has demonstrated a genetic link between *pcs* and *Btk29A* during oogenesis (Sinka et al., 2002). We have further gone on to show that reducing *Btk29A* levels maternally can also suppress the early patterning defects displayed by pcs^{gs} *mat* mutant embryos. This indicates that Btk29A is the major target of Pcs regulation during oogenesis.

However, the situation appears to be more complex during muscle development. We have shown that Btk29A is only expressed in a subset of mesodermal cells up to the time of FC specification, while Pcs is expressed panmesodermally at this time. In addition, Pcs is expressed during the rest of muscle development when Btk29A is absent. This suggests that Pcs must be acting independently of Btk29A. Indeed, genetic analysis does not support an interaction between *pcs* and *Btk29A* during muscle development. Therefore, we propose that, while Pcs may indeed regulate Btk29A activity in a subset of mesodermal cells early during muscle development, Pcs must have other targets. We hypothesize that these are other NRTKs and that the ability of Pcs to regulate multiple NRTKs at different times and places during development could account for its ability to regulate multiple processes. To support this hypothesis, a previous study has described expression of the NRTK Abl in differentiating muscles (Bennett and Hoffmann, 1992) and we have observed expression of both Src42A and Src64B throughout mesodermal patterning, FC specification, and muscle morphogenesis (K.B. and M.K.B., unpublished results). It is therefore likely that NRTKs play important roles in regulating multiple steps of muscle development. Further study of these important signaling molecules should yield new insights into how these processes are controlled.

Acknowledgments

We especially thank M. Erdelyi, S. Beckendorf, A. Ephrussi, R. Lehmann, and the Bloomington *Drosophila* Stock Center for generously providing fly strains and antibodies. We are grateful to J. Zallen, K. Anderson, R. Shapiro, and members of the Baylies laboratory for helpful discussions and critically reading the manuscript. M.B is supported by National Institutes of Health Grant GM56989.

Appendix A. Supplementary data

Supplementary data associated with this article can be found, in the online version, at doi:10.1016/j.ydbio.2006.07.049.

References

Artero, R.D., Castanon, I., Baylies, M.K., 2001. The immunoglobulin-like protein Hibris functions as a dose-dependent regulator of myoblast fusion and is differentially controlled by Ras and Notch signaling. Development 128, 4251–4264.

Artero, R., Furlong, E.E., Beckett, K., Scott, M.P., Baylies, M., 2003. Notch and Ras signaling pathway effector genes expressed in fusion competent and founder cells during *Drosophila* myogenesis. Development 130, 6257–6272.

Bate, M., 1990. The embryonic development of larval muscles in *Drosophila*. Development 110, 791–804.

Bate, M., Rushton, E., 1993. Myogenesis and muscle patterning in *Drosophila*. C. R. Acad. Sci. III 316, 1047–1061.

Baylies, M.K., Bate, M., 1996. Twist: a myogenic switch in *Drosophila*. Science 272, 1481–1484.

Baylies, M.K., Michelson, A.M., 2001. Invertebrate myogenesis: looking back to the future of muscle development. Curr. Opin. Genet. Dev. 11, 431–439.

Baylies, M.K., Martinez Arias, A., Bate, M., 1995. Wingless is required for the formation of a subset of muscle founder cells during *Drosophila* embryogenesis. Development 121, 3829–3837.

Baylies, M.K., Bate, M., Ruiz Gomez, M., 1998. Myogenesis: a view from *Drosophila*. Cell 93, 921–927.

Bennett, R.L., Hoffmann, F.M., 1992. Increased levels of the *Drosophila* Abelson tyrosine kinase in nerves and muscles: subcellular localization and mutant phenotypes imply a role in cell–cell interactions. Development 116, 953–966.

Borkowski, O.M., Brown, N.H., Bate, M., 1995. Anterior–posterior subdivision and the diversification of the mesoderm in *Drosophila*. Development 121, 4183–4193.

Bour, B.A., Chakravarti, M., West, J.M., Abmayr, S.M., 2000. *Drosophila* SNS, a member of the immunoglobulin superfamily that is essential for myoblast fusion. Genes Dev. 14, 1498–1511.

Brand, A.H., Perrimon, N., 1993. Targeted gene expression as a means of altering cell fates and generating dominant phenotypes. Development 118, 401–415.

Campos-Ortega, J.A., Hartenstein, V., 1995. The Embryonic Development of *Drosophila* melanogaster. Springer-Verlag, New York.

Carmena, A., Bate, M., Jimenez, F., 1995. Lethal of scute, a proneural gene, participates in the specification of muscle progenitors during *Drosophila* embryogenesis. Genes Dev. 9, 2373–2383.

Carmena, A., Gisselbrecht, S., Harrison, J., Jimenez, F., Michelson, A.M., 1998. Combinatorial signaling codes for the progressive determination of cell fates in the *Drosophila* embryonic mesoderm. Genes Dev. 12, 3910–3922.

Carmena, A., Buff, E., Halfon, M.S., Gisselbrecht, S., Jimenez, F., Baylies, M.K., Michelson, A.M., 2002. Reciprocal regulatory interactions between the Notch and Ras signaling pathways in the *Drosophila* embryonic mesoderm. Dev. Biol. 244, 226–242.

Chandrasekaran, V., Beckendorf, S.K., 2005. Tec29 controls actin remodeling and endoreplication during invagination of the *Drosophila* embryonic salivary glands. Development 132, 3515–3524.

Cox, V.T., Baylies, M.K., 2005. Specification of individual Slouch muscle progenitors in *Drosophila* requires sequential Wingless signaling. Development 132, 713–724.

Cox, V.T., Beckett, K., Baylies, M.K., 2005. Delivery of wingless to the ventral mesoderm by the developing central nervous system ensures proper patterning of individual slouch-positive muscle progenitors. Dev. Biol. 287, 403–415.

Doe, C.Q., Smouse, D., Goodman, C.S., 1988. Control of neuronal fate by the *Drosophila* segmentation gene even-skipped. Nature 333, 376–378.

Dohrmann, C., Azpiazu, N., Frasch, M., 1990. A new *Drosophila* homeo box gene is expressed in mesodermal precursor cells of distinct muscles during embryogenesis. Genes Dev. 4, 2098–2111.

Duan, H., Skeath, J.B., Nguyen, H.T., 2001. *Drosophila* Lame duck, a novel member of the Gli superfamily, acts as a key regulator of myogenesis by controlling fusion-competent myoblast development. Development 128, 4489–4500.

Dworak, H.A., Charles, M.A., Pellerano, L.B., Sink, H., 2001. Characterization of *Drosophila* hibris, a gene related to human nephrin. Development 128, 4265–4276.

Ephrussi, A., Dickinson, L.K., Lehmann, R., 1991. Oskar organizes the germ plasm and directs localization of the posterior determinant nanos. Cell 66, 37–50.

Estrada, B., Choe, S.E., Gisselbrecht, S.S., Michaud, S., Raj, L., Busser, B.W., Halfon, M.S., Church, G.M., Michelson, A.M., 2006. An integrated strategy for analyzing the unique developmental programs of different myoblast subtypes. PLoS Genet. 2, e16.

Frasch, M., 1999. Controls in patterning and diversification of somatic muscles during *Drosophila* embryogenesis. Curr. Opin. Genet. Dev. 9, 522–529.

Frasch, M., Hoey, T., Rushlow, C., Doyle, H., Levine, M., 1987. Characterization and localization of the even-skipped protein of *Drosophila*. EMBO J. 6, 749–759.

Furlong, E.E., Andersen, E.C., Null, B., White, K.P., Scott, M.P., 2001. Patterns of gene expression during *Drosophila* mesoderm development. Science 293, 1629–1633.

Gaul, U., Jackle, H., 1987. Pole region-dependent repression of the *Drosophila* gap gene Kruppel by maternal gene products. Cell 51, 549–555.

Gavis, E.R., Lehmann, R., 1992. Localization of nanos RNA controls embryonic polarity. Cell 71, 301–313.

Gonzalez, F., Swales, L., Bejsovec, A., Skaer, H., Martinez Arias, A., 1991. Secretion and movement of wingless protein in the epidermis of the *Drosophila* embryo. Mech. Dev. 35, 43–54.

Guarnieri, D.J., Dodson, G.S., Simon, M.A., 1998. SRC64 regulates the localization of a Tec-family kinase required for *Drosophila* ring canal growth. Mol. Cell 1, 831–840.

Halfon, M.S., Carmena, A., Gisselbrecht, S., Sackerson, C.M., Jimenez, F., Baylies, M.K., Michelson, A.M., 2000. Ras pathway specificity is determined by the integration of multiple signal-activated and tissue-restricted transcription factors. Cell 103, 63–74.

Jankovics, F., Sinka, R., Erdelyi, M., 2001. An interaction type of genetic screen reveals a role of the Rab11 gene in oskar mRNA localization in the developing *Drosophila melanogaster* oocyte. Genetics 158, 1177–1188.

Jankovics, F., Sinka, R., Lukacsovich, T., Erdelyi, M., 2002. MOESIN crosslinks actin and cell membrane in *Drosophila* oocytes and is required for OSKAR anchoring. Curr. Biol. 12, 2060–2065.

Johnstone, O., Lasko, P., 2001. Translational regulation and RNA localization in *Drosophila* oocytes and embryos. Annu. Rev. Genet. 35, 365–406.

Katzen, A.L., Kornberg, T., Bishop, J.M., 1990. Diverse expression of dsrc29A, a gene related to src, during the life cycle of *Drosophila melanogaster*. Development 110, 1169–1183.

Kim-Ha, J., Smith, J.L., Macdonald, P.M., 1991. Oskar mRNA is localized to the posterior pole of the *Drosophila* oocyte. Cell 66, 23–35.

Knirr, S., Frasch, M., 2001. Molecular integration of inductive and mesoderm-intrinsic inputs governs even-skipped enhancer activity in a subset of pericardial and dorsal muscle progenitors. Dev. Biol. 238, 13–26.

Lai, E.C., 2004. Notch signaling: control of cell communication and cell fate. Development 131, 965–973.

Lai, Z.C., Fortini, M.E., Rubin, G.M., 1991. The embryonic expression patterns of zfh-1 and zfh-2, two *Drosophila* genes encoding novel zinc-finger homeodomain proteins. Mech. Dev. 34, 123–134.

Lehmann, R., Nusslein-Volhard, C., 1991. The maternal gene nanos has a central role in posterior pattern formation of the *Drosophila* embryo. Development 112, 679–691.

Lewis, C.M., Broussard, C., Czar, M.J., Schwartzberg, P.L., 2001. Tec kinases: modulators of lymphocyte signaling and development. Curr. Opin. Immunol. 13, 317–325.

Macdonald, P.M., Ingham, P., Struhl, G., 1986. Isolation, structure, and expression of even-skipped: a second pair-rule gene of *Drosophila* containing a homeo box. Cell 47, 721–734.

Manseau, L.J., Schupbach, T., 1989. The egg came first, of course! Anterior–posterior pattern formation in *Drosophila* embryogenesis and oogenesis. Trends Genet. 5, 400–405.

Markussen, F.H., Michon, A.M., Breitwieser, W., Ephrussi, A., 1995. Translational control of oskar generates short OSK, the isoform that induces pole plasma assembly. Development 121, 3723–3732.

Matsushita, M., Yamadori, T., Kato, S., Takemoto, Y., Inazawa, J., Baba, Y., Hashimoto, S., Sekine, S., Arai, S., Kunikata, T., Kurimoto, M., Kishimoto, T., Tsukada, S., 1998. Identification and characterization of a novel SH3-domain binding protein, Sab, which preferentially associates with Bruton's tyrosine kinase (BtK). Biochem. Biophys. Res. Commun. 245, 337–343.

O'Neill, J.W., and Bier, E. (1994). Double-label in situ hybridization using biotin and digoxigenin-tagged RNA probes. BioTechniques 17, 870, 874–875.

Panin, V.M., Irvine, K.D., 1995. Modulators of Notch signaling. Semin. Cell Dev. Biol. 9, 609–617.

Piccin, A., Salameh, A., Benna, C., Sandrelli, F., Mazzotta, G., Zordan, M., Rosato, E., Kyriacou, C.P., Costa, R., 2001. Efficient and heritable functional knock-out of an adult phenotype in *Drosophila* using a GAL4-driven hairpin RNA incorporating a heterologous spacer. Nucleic Acids Res. 29, E55.

Ranganayakulu, G., Schulz, R.A., Olson, E.N., 1996. Wingless signaling induces nautilus expression in the ventral mesoderm of the *Drosophila* embryo. Dev. Biol. 176, 143–148.

Riechmann, V., Ephrussi, A., 2001. Axis formation during *Drosophila* oogenesis. Curr. Opin. Genet. Dev. 11, 374–383.

Roulier, E.M., Panzer, S., Beckendorf, S.K., 1998. The Tec29 tyrosine kinase is required during *Drosophila* embryogenesis and interacts with Src64 in ring canal development. Mol. Cell 1, 819–829.

Ruiz-Gomez, M., Romani, S., Hartmann, C., Jackle, H., Bate, M., 1997. Specific muscle identities are regulated by Kruppel during *Drosophila* embryogenesis. Development 124, 3407–3414.

Ruiz-Gomez, M., Coutts, N., Price, A., Taylor, M.V., Bate, M., 2000. *Drosophila* dumbfounded: a myoblast attractant essential for fusion. Cell 102, 189–198.

Ruiz-Gomez, M., Coutts, N., Suster, M.L., Landgraf, M., Bate, M., 2002. Myoblasts incompetent encodes a zinc finger transcription factor required to specify fusion-competent myoblasts in *Drosophila*. Development 129, 133–141.

Simon, M.A., 2000. Receptor tyrosine kinases: specific outcomes from general signals. Cell 103, 13–15.

Sinka, R., Jankovics, F., Somogyi, K., Szlanka, T., Lukacsovich, T., Erdelyi, M., 2002. poirot, a new regulatory gene of *Drosophila* oskar acts at the level of the short Oskar protein isoform. Development 129, 3469–3478.

Smith, C.I., Islam, T.C., Mattsson, P.T., Mohamed, A.J., Nore, B.F., Vihinen, M., 2001. The Tec family of cytoplasmic tyrosine kinases: mammalian Btk, Bmx, Itk, Tec, Txk and homologs in other species. BioEssays 23, 436–446.

Tateno, M., Nishida, Y., Adachi-Yamada, T., 2000. Regulation of JNK by Src during *Drosophila* development. Science 287, 324–327.

Thisse, B., el Messal, M., Perrin-Schmitt, F., 1987. The twist gene: isolation of a *Drosophila* zygotic gene necessary for the establishment of dorsoventral pattern. Nucleic Acids Res. 15, 3439–3453.

Thomas, J.H., Wieschaus, E., 2004. src64 and tec29 are required for microfilament contraction during *Drosophila* cellularization. Development 131, 863–871.

Tsygankov, A.Y., 2003. Non-receptor protein tyrosine kinases. Front. Biosci. 8, s595–s635.

van de Wetering, M., Cavallo, R., Dooijes, D., van Beest, M., van Es, J., Loureiro, J., Ypma, A., Hursh, D., Jones, T., Bejsovec, A., Peifer, M., Mortin, M., Clevers, H., 1997. Armadillo coactivates transcription driven by the product of the *Drosophila* segment polarity gene dTCF. Cell 88, 789–799.

Vincent III, W.S., Gregory, R.J., Wadsworth, S.C., 1989. Embryonic expression of a *Drosophila* src gene: alternate forms of the protein are expressed in segmental stripes and in the nervous system. Genes Dev. 3, 334–347.

Wadsworth, S.C., Muckenthaler, F.A., Vincent III, W.S., 1990. Differential expression of alternate forms of a *Drosophila* src protein during embryonic and larval tissue differentiation. Dev. Biol. 138, 296–312.

Wang, C., Lehmann, R., 1991. Nanos is the localized posterior determinant in *Drosophila*. Cell 66, 637–647.

Wang, C., Dickinson, L.K., Lehmann, R., 1994. Genetics of nanos localization in *Drosophila*. Dev. Dyn. 199, 103–115.

Wu, X., Golden, K., Bodmer, R., 1995. Heart development in *Drosophila* requires the segment polarity gene wingless. Dev. Biol. 169, 619–628.

Yamadori, T., Baba, Y., Matsushita, M., Hashimoto, S., Kurosaki, M., Kurosaki, T., Kishimoto, T., Tsukada, S., 1999. Bruton's tyrosine kinase activity is negatively regulated by Sab, the Btk-SH3 domain-binding protein. Proc. Natl. Acad. Sci. U. S. A. 96, 6341–6346.